Neutron Resonance Spectroscopy. III. Th^{232} and U^{238}†

J. B. GARG, J. RAINWATER, J. S. PETERSEN,* AND W. W. HAVENS, JR.
Columbia University, New York, New York
(Received 17 January 1964)

The neutron total cross sections for Th^{232} and U^{238} have been measured from about 100 eV to 4 keV with ~0.5 nsec/m resolution at the highest energies. The mean level spacings for these nuclei have been observed to be (17.5±0.7) eV and (17.7±0.7) eV. For U^{238} about 17% of the observed levels probably belong to $l=1$ and are omitted from the statistical analysis of the data. S-wave strength functions of $(0.69\pm0.07)\times10^{-4}$ and $(0.90\pm0.10)\times10^{-4}$ are obtained for Th^{232} and U^{238}, respectively. Detailed comparisons of the observed statistical aspects of the level spacings and neutron reduced width distributions have been made with the predictions of various theoretical models. The distributions of Γ_n^0 for both nuclei seem to be consistent with a single-channel Porter-Thomas distribution. The observed distributions of nearest- and next-nearest-neighbor level spacings agree quite well with the expected distributions for real symmetric Hamiltonian matrices with randomly distributed matrix elements. The correlation coefficients for Th^{232} and U^{238} are, respectively: (a) (-0.21 ± 0.07) and (-0.26 ± 0.08) for adjacent level spacings, (b) (-0.03 ± 0.07) and (-0.17 ± 0.07) for adjacent reduced neutron widths, and (c) (0.12 ± 0.07) and (0.15 ± 0.07) for the neutron reduced width of a level and the average of its spacing from adjacent levels.

1. INTRODUCTION

THIS is the third of a series of papers presenting results obtained using time-of-flight neutron spectroscopy in conjunction with the Nevis synchrocyclotron as a pulsed neutron source. The two preceding papers[1,2] of this series gave results for U^{238}, Au, Ag, and Ta using a 35-m flight path and self-indication techniques for which a sample of the element is placed at the sample position and the resonance capture γ rays are detected by a scintillation counter system.[3] Measurement of the counting rate (above background) versus neutron energy, with and without various thicknesses of a transmission sample of the same material in the neutron path, provides an effective technique for obtaining neutron resonance energies and level parameters for samples which have more capture than scattering at resonance and are not strong radioactive γ-ray sources. The spectrometer[4] now uses a 200-m flight path. A large detector consisting of a 15-kg slab of B^{10} (1.5×12×48 in.) is viewed by a bank of NaI detectors to detect the 480-keV photons following neutron capture in B^{10}. In addition to achieving about a factor 10 improvement in the energy resolution, the present system permits the measurement of total cross sections between resonances, and the study of resonances which have $\Gamma_n \gg \Gamma_\gamma$ (mainly scattering).

Th^{232} and U^{238} (natural abundance Th and U samples) have been selected as the first elements for which analysis of the results have been completed for a number of reasons. The interest in U^{238} and Th^{232} for the production of Pu^{239} and U^{233} for nuclear reactors is obvious. The interest in the measurements on these isotopes for physics lies partly in obtaining accurate experimental information on the neutron interactions *per se*. Of more current interest is the study of the systematics of the results in order to test theoretical models for the statistical properties of neutron processes and to inspire further theoretical advances. The quantities of interest include: (a) the $l=0$ strength function

$$S_0 \equiv \frac{\langle \Gamma_n^0 \rangle}{\langle D \rangle} = \frac{1}{E_{\max}} \sum_j (\Gamma_n^0)_j, \quad (1)$$

where $(\Gamma_n^0)_j = (\Gamma_n)_j (1\text{ eV}/E_j)^{1/2}$, and the sum is taken over all observed ($l=0$) levels to $E_{\max}$, (b) the distribution of the observed Γ_n^0 values about the mean $\langle \Gamma_n^0 \rangle$, (c) the distribution of nearest level spacings D about the mean spacing $\langle D \rangle$, (d) higher correlation effects in level spacings distributions such as the correlation of adjacent level spacings, etc., (e) correlations between adjacent Γ_n^0 values or between each Γ_n^0 value and the average of the two nearest-neighbor spacings involving that level, etc.

For such statistical tests it is important to have a very large number of levels belonging to a single population (ensemble) and to have the experimental values as free as possible from errors. Th^{232} and U^{238} are particularly useful test nuclei for this purpose. Natural Th is 100% Th^{232} while natural U is >99% U^{238} and is available in the required quantities for our measurements. These are both even-even, $J=0$, isotopes having a favorable level spacing and strength for $l=0$ resonance levels in the region from zero neutron energy to a few keV. The resonances are all $(\frac{1}{2}+)$ states of Th^{233} or U^{239}, except that a few of the observed very weak levels are probably "relatively strong" $l=1$ resonances. The experimental problem of obtaining reliable evidence concerning the systematics for a large number of levels is usually underestimated by those persons

† Work supported in part by the U. S. Atomic Energy Commission.
* Work performed during a visit from the Danish Atomic Energy Commission, Risö, Denmark.
[1] J. L. Rosen, J. S. Desjardins, J. Rainwater, and W. W. Havens, Jr., Phys. Rev. **118**, 687 (1960).
[2] J. S. Desjardins, J. L. Rosen, W. W. Havens, Jr., and J. Rainwater, Phys. Rev. **120**, 2114 (1960).
[3] J. Rainwater, W. W. Havens, Jr., J. S. Desjardins, and J. L. Rosen, Rev. Sci. Instr. **31**, 490 (1960).
[4] J. Rainwater, W. W. Havens, Jr., and J. B. Garg, Rev. Sci. Instr. **35**, 263 (1964).

not actively involved in such measurements. While strong levels in the lower part of the energy range are spectacularly evident and unambiguous, there is always some energy-dependent threshold of level strength which is apt to be discounted as just being due to a statistical fluctuation in the data. Similarly, a statistical fluctuation in the data may be mistakenly treated as a resonance. At higher energies there will be an increasing chance of counting two or more unresolved levels as one level. One must thus resist the temptation to extend the energy region included beyond that which can be treated reliably and must obtain large count numbers for good statistical accuracy.

The earlier 35-m Columbia results[1] on U^{238} were limited to level systematics in the region below 1 keV and were by far the best available at that time. Since then Firk, Lynn, and Moxon[5] have published results for U^{238} using the Harwell 15-MeV electron Linac and a 55-m flight path. Their resolution was significantly better than that for our 35-m measurements, but was at least a factor of 5 poorer than our present measurements. They have presented level systematics to about 1800 eV, except for a gap of $\sim$50 eV near 1600 eV. In view of the problem of level identification for weak levels, it is of interest to test the level assignments of the Harwell and the earlier Columbia results against those of the much improved present measurements. Below 1000 eV the agreement of the 3 sets of results is good, with differences in only a few marginal cases. Above 1000 eV we agree generally with the Harwell results for the identification of the strong levels, but a rather large number of their weaker levels seem to be statistical fluctuations in the data. The Harwell group has reported[6] preliminary results for Th to 1300 eV with an energy resolution closer to that of our present measurements and the agreement in the identification of levels in the two measurements is excellent.

For a given time-of-flight resolution, the energy resolution width, ΔE, increases as $E^{3/2}$. Our factor of about 10 times improvements in the time-of-flight resolution thus permits only a factor of $\sim$4 increase in $E_{\max}$ for the same ΔE. To be conservative, we have thus limited our analysis of level systematics for Th^{232} and U^{238} to $E<4$ keV.

2. EXPERIMENTAL MEASUREMENTS

A detailed account of the present experimental arrangement and general operating procedures is given elsewhere.[4] The reported measurements on Th were all made during January 1962 and those for U^{238} during January 1963. In each case a large number of other elements were also investigated, partly to aid in an over-all evaluation of the operation of the system for purposes of analysis and as a guide for system improvements. The effective flight path length, about 201.5 m in each case, is believed to be known to within 1 cm. The timing corresponding to each 0.1 μsec or wider detection channel, including the evaluation of the $t=0$ time-of-flight position, was known to within 0.1 μsec or better. The NaI detectors were placed directly behind the B^{10}-detector slab during all of Th and U measurements.

During the 1963 measurements a thick Pb shield was used above, below, and at the sides of the NaI detectors to reduce the cyclotron off background rate. A fast chopper was used for most of these measurements. The function of the fast chopper is to pass the burst of neutrons of the energy range being studied, and then close during the time of transit of these neutrons to the 200-m position. In this way the detectors are isolated from the strong gamma-ray background from the cyclotron chamber while counting those neutrons which have energies in the selected range. Its maximum open phasing was chosen in each case to favor passage of neutrons in the energy range being covered. For neutron energies $<$200 eV the fast chopper was removed from the beam and a slow chopper was used to perform the same function during a relatively short counting period at the end of the 1963 run. This mode of operation gave a much better low-energy counting rate and useful to background count ratio than was obtained using the fast chopper. However, our measurements in this energy region were of short duration. Hence the statistical accuracy of the data was not good enough to obtain reliable values for the resonance parameters.

For Th the energy interval was divided into four overlapping regions: from 50 to 200 eV, 80 to 350 eV, 300 to 1200 eV, and 1100 to 4000 eV. Detection channel widths for the 2000 channel analyzer were 0.8, 0.4, 0.2, and 0.1 μsec, respectively. The similar energy intervals for U were 35 to 213 eV, 200 to 600 eV, 600 to 1300 eV, and 1300 to 4000 eV, with detection channel widths of 0.8, 0.2, 0.1, and 0.1 μsec, respectively. In each case the fast neutron burst width was $<$0.1 μsec, so this was not the main limiting factor. The effective moderation time varies as $E^{-1/2}$ for moderated neutrons of energy E, and is $\sim$0.1 μsec near 1 keV. Near 4 keV the over-all effective experimental resolution width was about 6 eV ($\frac{1}{3}$ of the mean level spacing). Hence levels spaced by less than 6 eV would not appear as two peaks, but the observed linewidth might be too large for a single resonance, thereby suggesting that two (or more) levels are present. The theoretically favored level spacing distribution function predicts that $<$10% of the $l=0$ level spacings should be $<$6 eV for Th and U.

Three sample thicknesses of Th metal were used having $(1/n)$ values of 17.4, 51.8, and 174 b/atom. Five sample thicknesses of natural abundance U were used with $(1/n)$ values of 11.8, 41.2, 150, 236, and 590 b/atom. The thickest samples gave the main informa-

[5] F. W. K. Firk, J. E. Lynn, and M. C. Moxon, Nucl. Phys. 41, 614 (1963).

[6] C. A. Utley and R. H. Jones, Harwell Progress Report, AERE-PR/NP-2 (unpublished).

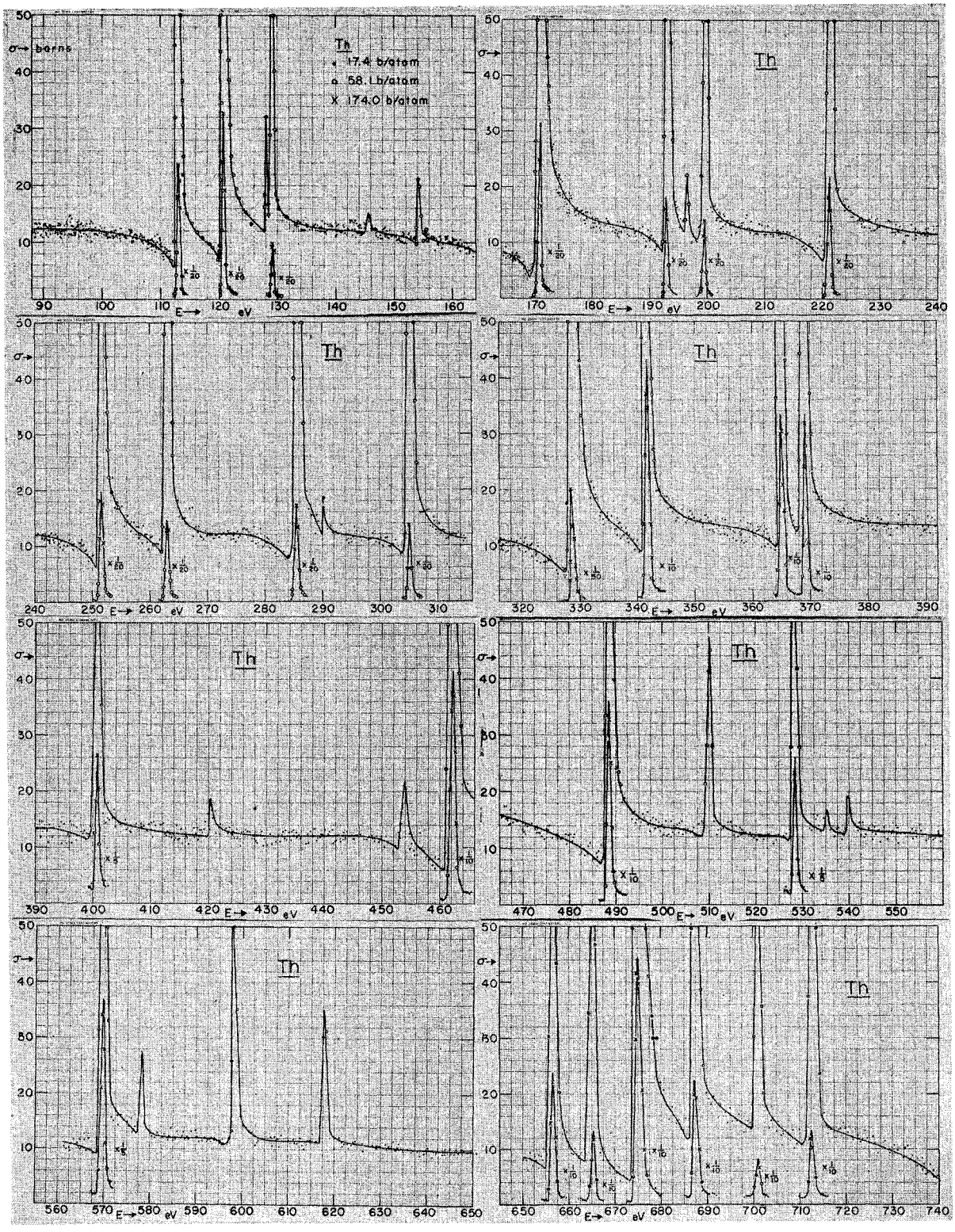

FIG. 1. The "measured" total neutron cross section of Th^{232} versus neutron energy. The peak values at resonances are limited by Doppler level broadening, experimental energy resolution, and the size of the $1/n$ value for our thinnest sample. Areas under these curves for the resonances may be quite different from the area under a true σ versus E plot.

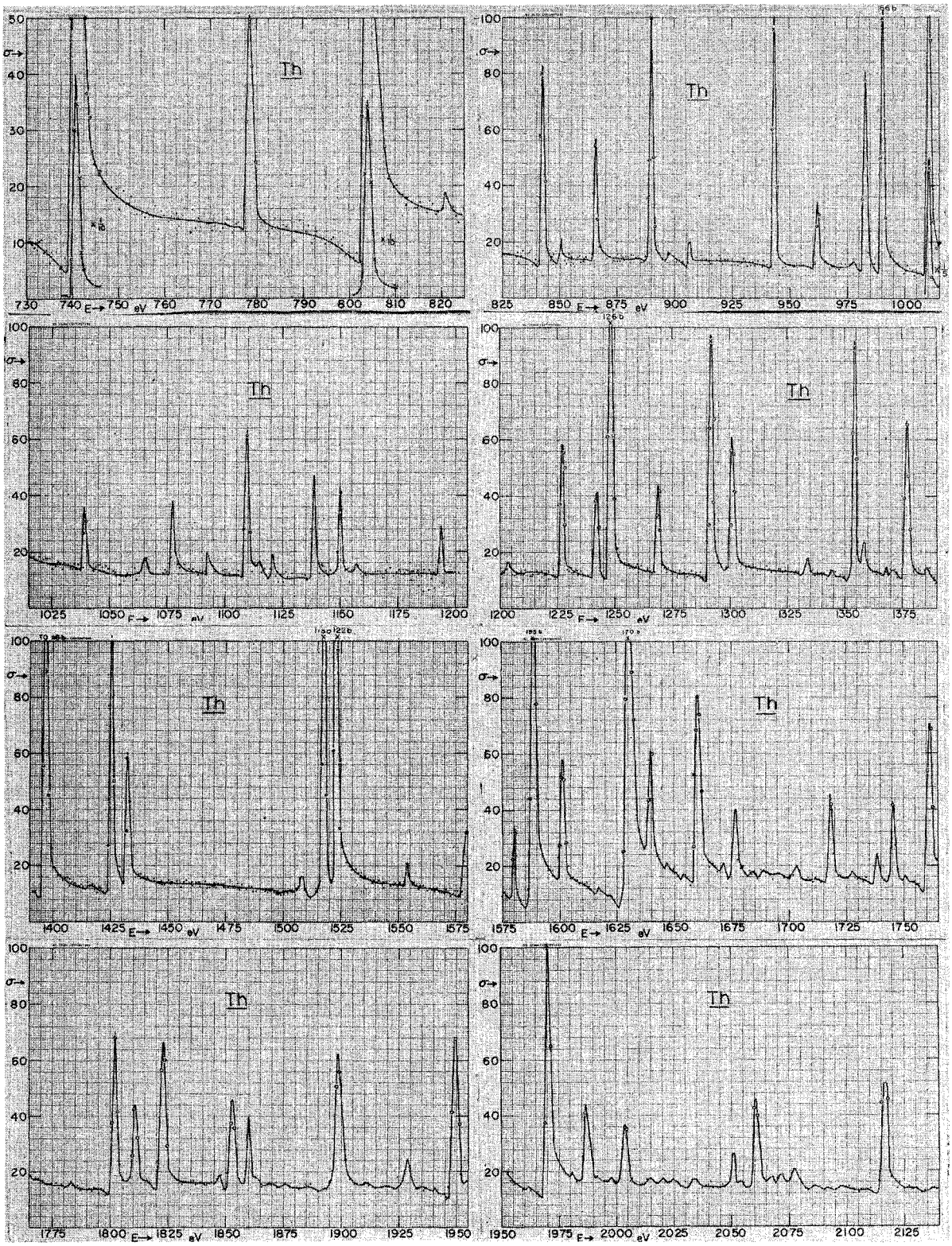

FIG. 1 (*continued*)

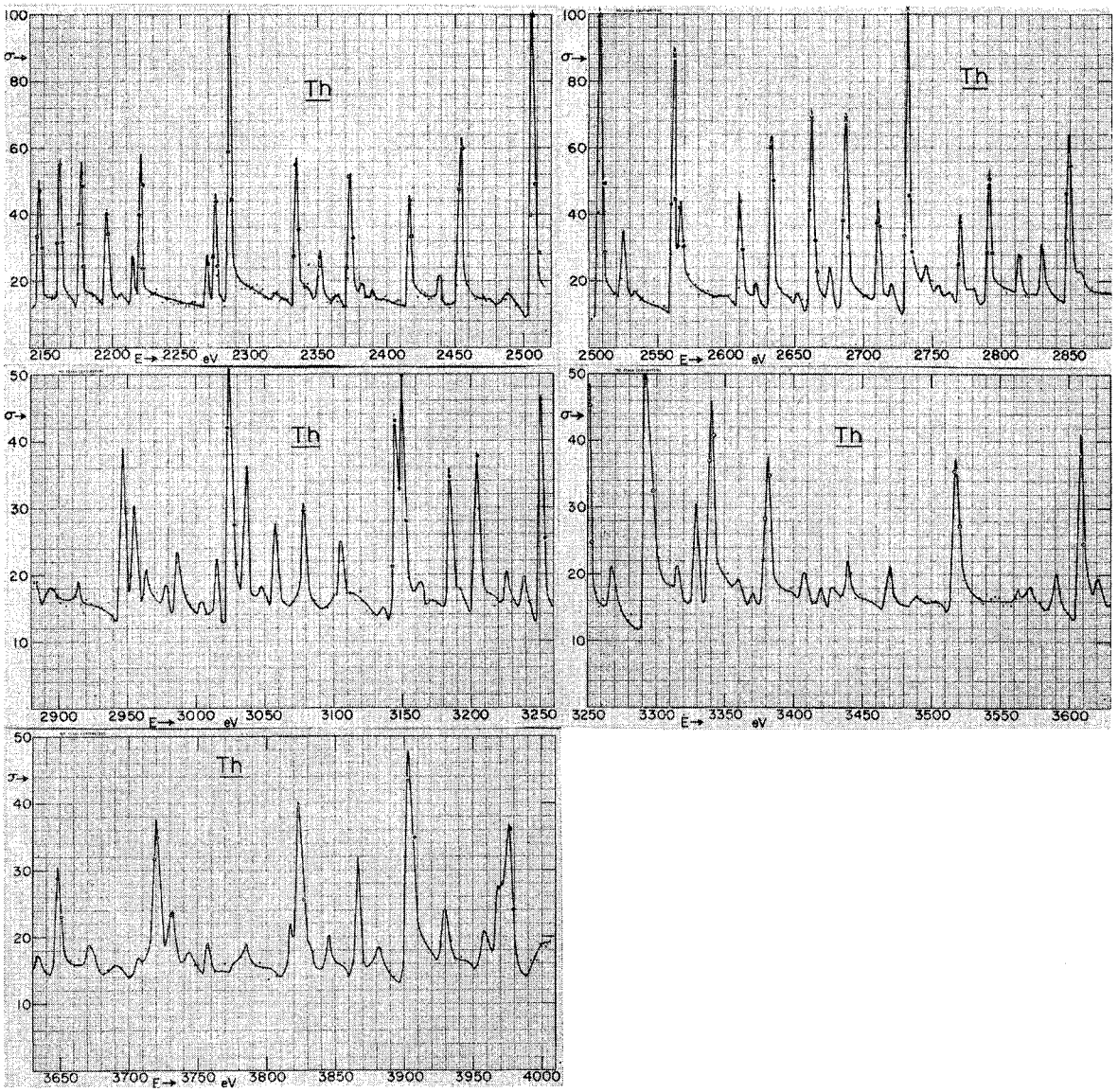

FIG. 1 (*continued*)

tion concerning the cross section away from resonances and information for the very weak levels. The thinnest samples were still quite thick ($1/n \ll \sigma_{max}$) for the strong levels, particularly at the low-energy end of the region studied.

About 10^7 total "sample in" counts, for all sample thicknesses and for 2000 channels, were obtained for Th for each of the three highest energy regions. Similar total "sample in" counts of 4 to 8×10^6 were obtained for the three upper energy regions for U. To evaluate the background count for each sample thickness and energy, we obtain the cyclotron off counting rate per channel and make use of the systematics of the counting rates at the bottom of saturated resonance dips ($T=0$) for Th, U, and the other elements studied at the same time. This procedure is described in more detail elsewhere.[4]

After the initial stages of data processing the expected background count was subtracted from the "open" and "sample in" count values. The counts were then normalized to the same effective cyclotron intensity times time. The correction[4] was next made to cancel the effects of "after burst" fast neutron production in 0.2-μsec interval spacings after deflection. Neutron transmission values and "experimental total cross section" σ values were calculated for each channel using IBM 650 or 1620 computers, where

$$\sigma_{exp} = -(1/n)\ln T_{exp}. \quad (2)$$

Figure 1 shows the observed σ versus E values for

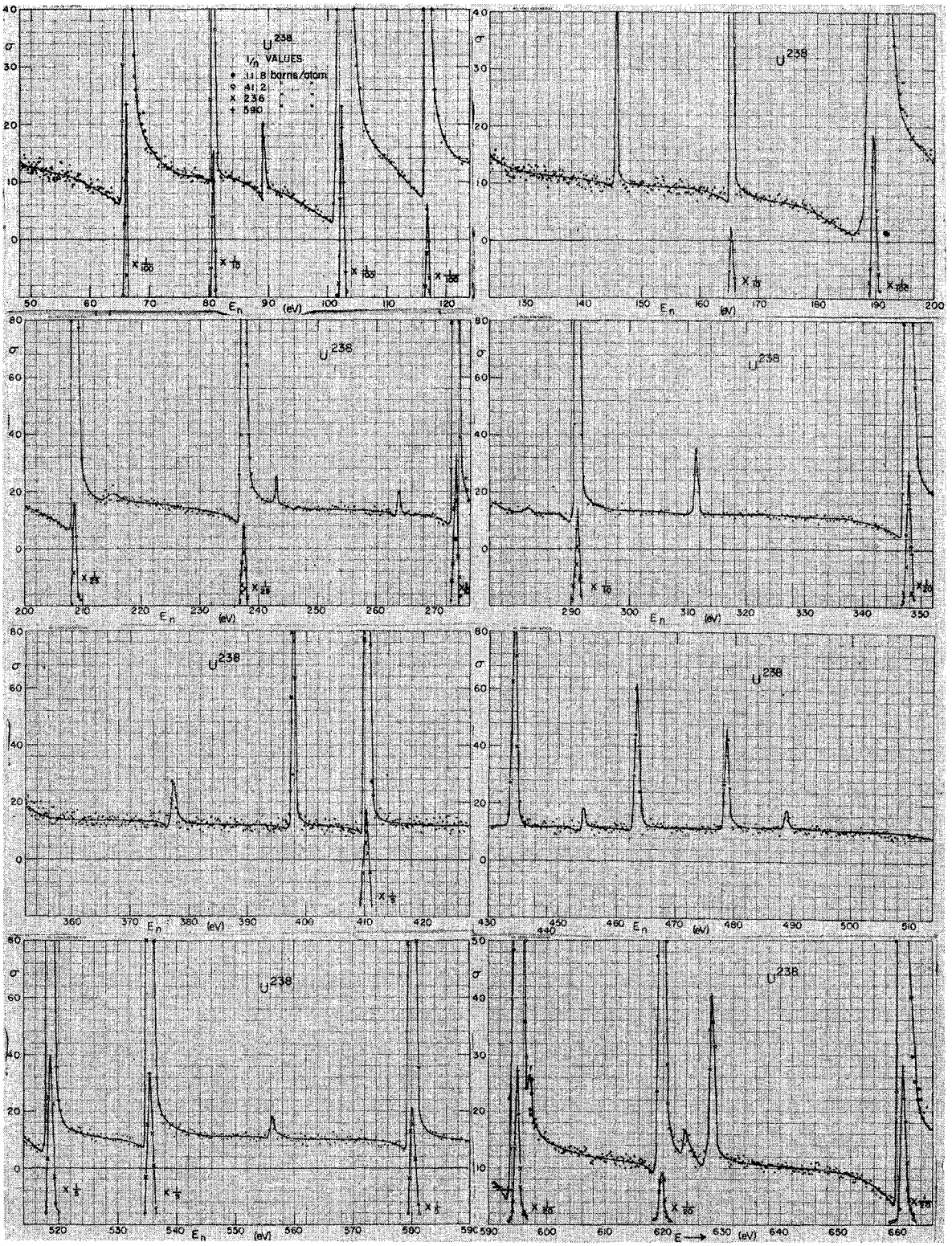

FIG. 2. The "measured" total cross section of U^{238} versus neutron energy.

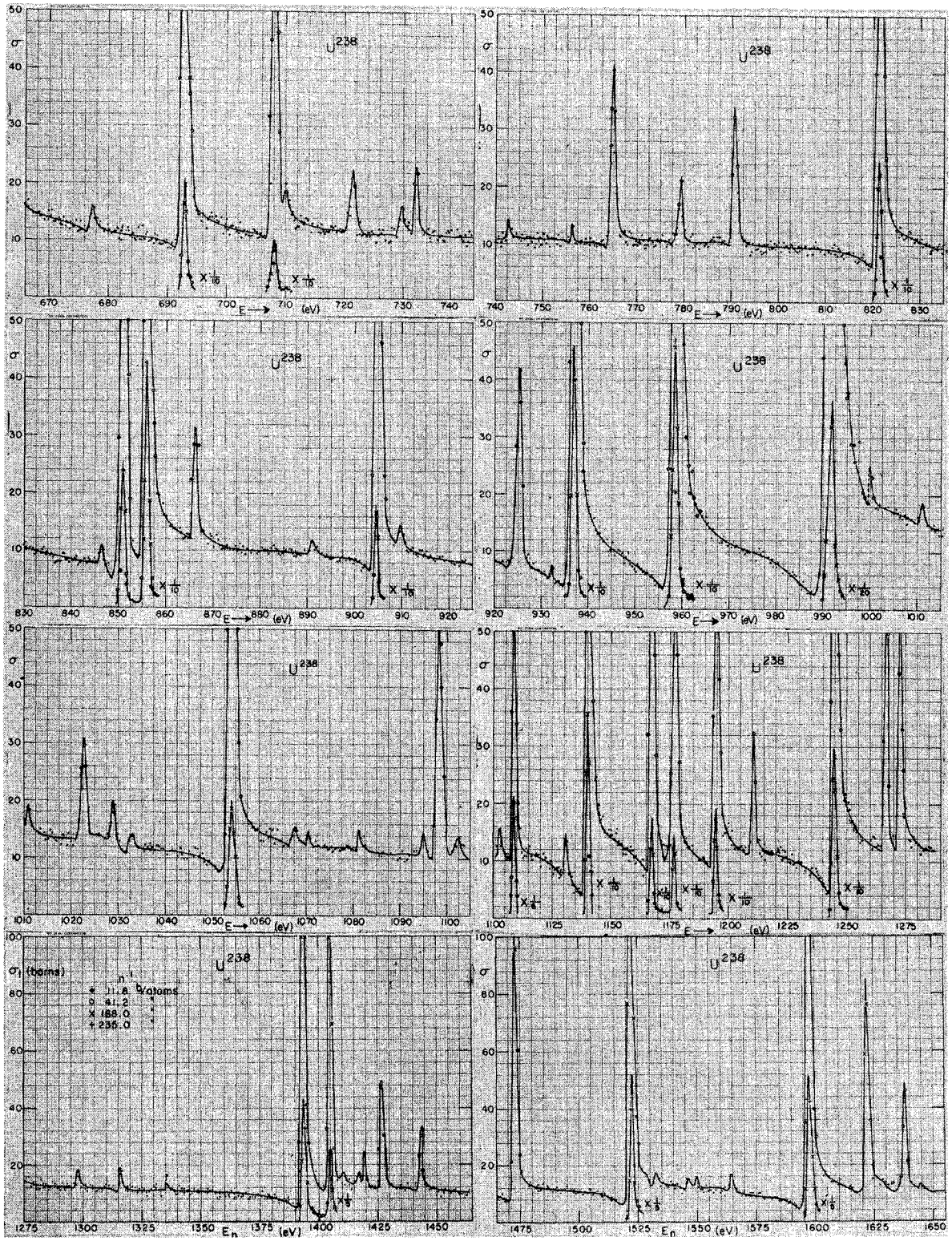

FIG. 2 (*continued*)

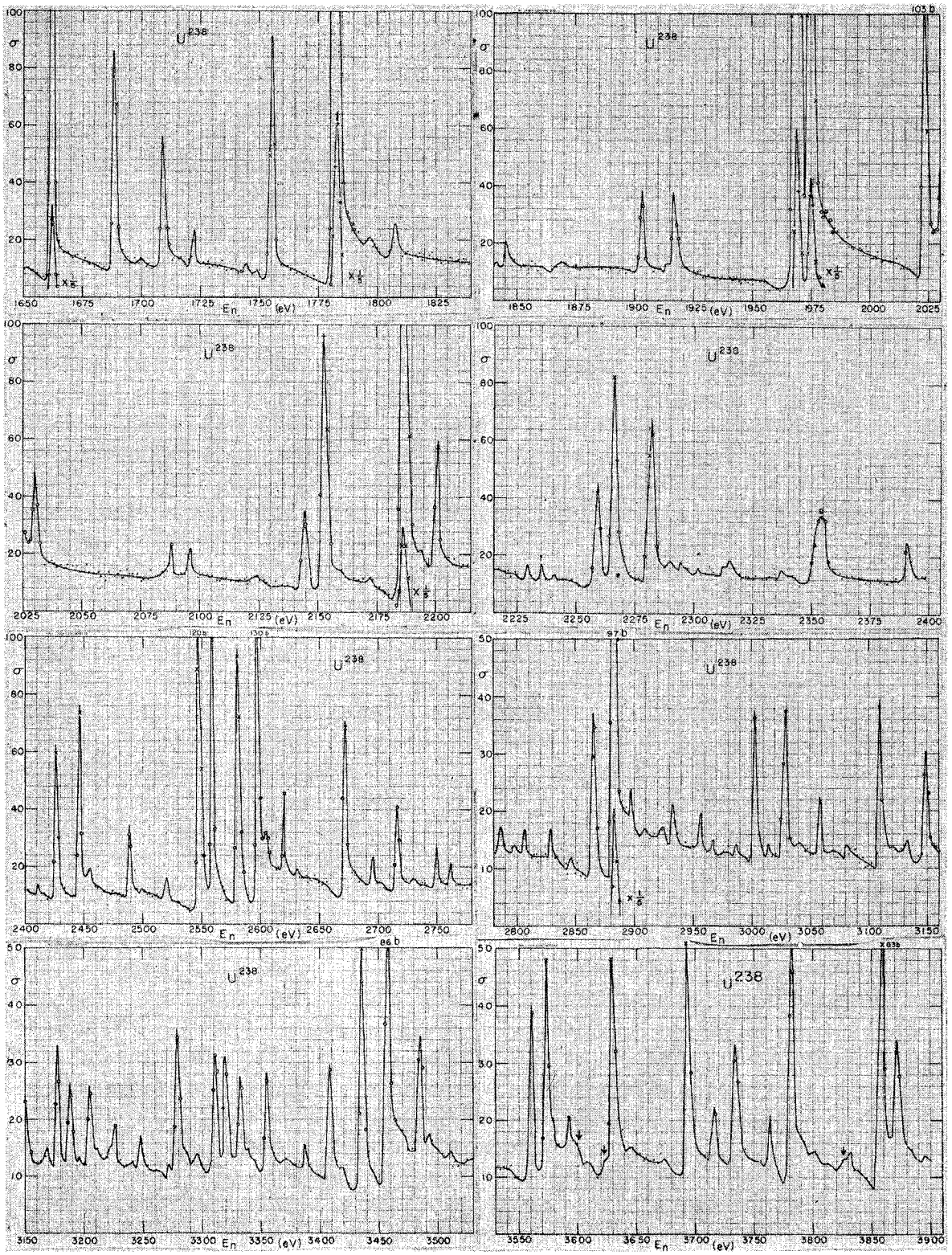

FIG. 2 (*continued*)

Th^{232} and Fig. 2 shows the similar results for U^{238}. The effect of the small U^{235} content of the uranium samples is not believed to be important in affecting the results for U^{238}. The indicated σ values use the transmission results for the thickest samples between levels, with a progression to thinner and thinner sample results as σ approaches large resonance values. For the weak levels the cross sections are mainly based on the thickest sample data. These curves reflect the effects of the experimental resolution width, the Doppler level broadening, the statistical counting uncertainty, and the choice of $(1/n)$ sample values. The indicated peak cross section values at resonance may be considerably smaller than the true Doppler broadened peak cross sections. The measured peak cross sections for the strong lower energy resonances are strongly limited by the fact that the thinnest samples are still relatively thick $(1/n \ll \sigma_{\max})$.

Table I for Th^{232}, and Table II for U^{238}, list the resonance energies and their uncertainties, usually taken as one timing channel. A comparison of our Th energies with those measured by Utley and Jones[6] at Harwell shows that our values are systematically higher than theirs by about 0.1% which corresponds to a 0.05% μsec/m time-of-flight difference. The present U^{238} resonance energies are lower than those obtained in the Columbia 35-m measurements[1] by $\sim$0.1% at 100 eV to $\sim$0.5% at 1 keV. This suggests that there was a one-channel error in the $t=0$ assignment for the 35-m measurements. The U^{238} energies agree to $\sim$0.1% with those of Firk *et al.*[5] at 100 eV, but the Harwell values are somewhat erratically higher above 1 keV, averaging $\sim$1% higher near 1500 eV. This suggests a $t=0$ error in their time-of-flight scale for those measurements.

3. ANALYSIS FOR RESONANCE PARAMETERS

The most tedious and difficult part of the data processing is the analysis for the determination of resonance parameters. When only scattering and capture are present this involves determining the neutron width Γ_n (or Γ_n^0), and, if possible, the capture width Γ_γ. For Th^{232} and U^{238} the $l=0$ resonances only involve $(\frac{1}{2}+)$ states so the extra complication of attempting to determine the compound nucleus spin is absent. When the interference term between potential and resonance scattering cannot be neglected, but the resonance energy is a few keV or less, the single level Breit-Wigner formula may be written with good accuracy in the form

$$\sigma(x)=\frac{\sigma_0}{1+x^2}+\frac{2\sigma_0(R/\lambda\!\!\!^{-})}{1+x^2}+4\pi R^2. \tag{3}$$

$\sigma_0=4\pi\lambda\!\!\!^{-2}(g\Gamma_n/\Gamma)$ is the total resonance cross section at exact resonance energy E_0. The spin factor, g, is unity in this case. Γ is the total level width, and $x=2(E-E_0)/\Gamma$. The potential scattering cross section $4\pi R^2$ is influenced by the wing contributions from the neighboring levels and is, in principle, slightly energy-dependent in the region of each resonance, and slightly different for each level. The factor $2\pi\lambda\!\!\!^{-}$ is the de Broglie wavelength of the neutron in the center-of-mass system. It is customary to use the neutron energy in the laboratory system rather than in the center-of-mass system.

The Doppler broadening of the resonance due to the thermal motion of the atoms gives, in gas theory approximation,

$$\sigma(x)=\sigma_0\psi(\beta,x)+2\sigma_0(R/\lambda\!\!\!^{-})\varphi(\beta,x)+4\pi R^2, \tag{4}$$

where

$$\psi(\beta,x)=(\pi^{1/2}\beta)^{-1}\int_{-\infty}^{\infty}\frac{dy}{1+y^2}\exp\left\{-\frac{(x-y)^2}{\beta^2}\right\}, \tag{5a}$$

$$\varphi(\beta,x)=(\pi^{1/2}\beta)^{-1}\int_{-\infty}^{\infty}\frac{ydy}{1+y^2}\exp\left\{-\frac{(x-y)^2}{\beta^2}\right\}. \tag{5b}$$

Here $\beta=2\Delta/\Gamma$, and $\Delta=2(kTE_0/M)^{1/2}$ [$\approx(E_0/10M)^{1/2}$ eV at normal room temperature] is the Doppler width. M is the atomic mass in units of the neutron mass, and kT is the effective sample temperature in energy units. The interference term $\varphi(\beta,x)$ was not included in the earlier Columbia 35-m data analysis[1,2] since the self-indication method discriminates against the level wing regions, is based on the effect of the capture term only for detection, and is only useful when Γ_n is not large compared with Γ_γ. The omission of the interference term is not expected to have introduced serious errors in the analysis of the earlier self-indication measurements.[1]

Analysis for the determination of resonance parameters is best made in terms of the measured transmission curves for the present type of measurements. If the experimental resolution function is known with adequate precision, the most elegant method is to use an electronic computer, such as the IBM 7094, to calculate the predicted transmission curves for various choices of E_0, Γ_n, Γ, and R values, with Doppler broadening included, and with the experimental resolution function and the effect of adjacent levels folded in. A least-square analysis can then determine the best fitting values for the parameters. Such procedures have been developed but they are quite complicated and the analysis is expensive in terms of computer time, partly since the computer evaluates $\psi(\beta,x)$ and $\varphi(\beta,x)$ at each point as needed. Moreover, the usefulness of this analysis is limited by the accuracy with which the over-all instrumental resolution function is known. Unfortunately, this quantity is not known very accurately at the present time. Consequently we use the simpler analysis based on the area, A, under the transmission dip. If the experimental transmission curve is divided by the transmission, T_p, due to potential scattering and the effect of the wings of adjacent resonances, the resulting transmission curve $T'(E)$ includes only the effects

TABLE I. Neutron resonance level parameters of Th^{232}.[a]

E_0 (eV)	ΔE_0	Γ_n^0 (meV)	$\Delta\Gamma_n^0$	Γ_γ (meV)
21.84		0.38	0.04	21.5
23.48		0.66	0.040	25
59.55		0.60	0.13	20.8
69.20		5.1	0.2	18.4
112.90	0.08	1.13	0.20	15±3
120.73	0.10	1.69	0.20	20±5
128.00	0.10	0.01	0.004	
129.08	0.10	0.30	0.05	
145.92	0.10	0.003	0.001	
154.34	0.10	0.01	0.002	
170.40	0.20	4.45	0.4	
192.56	0.15	1.08	0.15	
196.00	0.16	0.025	0.003	
199.19	0.16	0.78	0.14	
220.98	0.18	2.10	0.20	16±5
251.29	0.20	2.00	0.20	22±3
263.18	0.25	1.17	0.12	
285.61	0.25	1.66	0.15	17±5
305.27	0.30	1.50	0.20	16±6
328.75	0.20	3.80	0.30	20±10
341.90	0.20	1.95	0.10	
365.06	0.20	1.46	0.10	22±4
369.31	0.20	1.45	0.10	25±5
400.82	0.25	0.50	0.05	
420.70	0.25	0.01	0.005	
454.34	0.30	0.04	0.02	
462.42	0.30	2.89	0.20	30±20
488.61	0.30	2.70	0.20	30±20
510.68	0.35	0.22	0.04	
528.57	0.35	0.70	0.10	
534.75	0.35	0.01	0.01	
540.10	0.35	0.03	0.01	
569.89	0.40	1.05	0.05	
578.19	0.40	0.08	0.02	
598.17	0.40	0.37	0.03	
617.93	0.45	0.15	0.03	
656.79	0.45	1.85	0.30	
665.19	0.45	0.75	0.05	
675.19	0.50	8.00	0.50	32±15
687.40	0.50	2.40	0.20	
700.96	0.50	0.60	0.05	
712.83	0.55	1.20	0.30	28±8
740.80	0.55	8.00	0.50	23±22
778.74	0.55	0.40	0.05	
804.42	0.60	7.00	1.00	35±55
821.61	0.60	0.02	0.005	
842.70	0.60	0.95	0.05	
850.82	0.65	0.02	0.01	
866.71	0.65	0.50	0.03	
890.30	0.70	1.10	0.10	
897.20	0.70	0.01	0.01	
906.57	0.70	0.06	0.02	
943.65	0.75	1.20	0.30	
963.05	0.75	0.20	0.04	
983.05	0.80	0.95	0.20	
990.71	0.85	2.40	0.25	
1010.70	0.90	4.70	0.30	
1039.54	0.90	0.45	0.05	
1065.80	0.95	0.10	0.03	
1077.36	1.00	0.36	0.08	
1093.06	1.00	0.12	0.02	
1110.13	1.05	0.84	0.03	
1122.42	1.05	0.04	0.02	
1139.13	1.05	0.41	0.05	
1150.83	1.10	0.70	0.05	
1156.7	1.10	0.03	0.02	
1194.20	1.10	0.16	0.02	
1204.47	0.60	0.03	0.01	
1227.76	0.60	0.62	0.05	
1243.26	0.60	0.42	0.04	
1248.69	0.60	2.10	0.10	
1269.55	0.60	0.47	0.04	
1292.21	0.60	1.70	0.20	
1301.83	0.60	0.98	0.05	
1334.68	0.60	0.07	0.02	
1345.46	0.60	0.02	0.01	
1354.99	0.65	1.50	0.20	
1359.80	0.65	0.10	0.02	
1377.88	0.65	0.95	0.05	
1387.05	0.65	0.04	0.02	
1397.75	0.65	2.00	0.20	
1416.59	0.65	0.02	0.01	
1426.90	0.65	1.65	0.20	
1433.58	0.70	0.85	0.10	
1509.51	0.70	0.06	0.03	
1518.40	0.70	2.85	0.20	
1524.11	0.70	2.70	0.20	
1555.63	0.75	0.120	0.04	
1581.21	0.75	0.25	0.04	
1589.01	0.75	5.20	0.40	
1603.02	0.80	0.95	0.10	
1630.69	0.80	7.50	0.5	
1640.68	0.80	1.00	0.15	
1660.94	0.85	1.90	0.20	
1672.30	0.85	0.04	0.02	
1677.79	0.85	0.46	0.04	
1705.50	0.90	0.12	0.06	
1720.09	0.90	0.72	0.04	
1728.20	0.90	0.04	0.02	
1739.85	0.95	0.15	0.03	
1746.85	0.95	0.62	0.04	
1763.00	1.00	1.85	0.15	
1803.31	1.00	1.50	0.15	
1811.75	1.05	0.95	0.05	
1823.46	1.10	1.70	0.20	
1848.60	1.10	0.05	0.02	
1853.76	1.10	0.80	0.10	
1861.46	1.15	0.68	0.05	
1900.66	1.15	2.20	0.2	
1930.59	1.20	0.42	0.04	
1950.54	1.20	1.80	0.2	
1970.81	1.20	3.50	0.5	
1987.73	1.20	1.20	0.10	
2004.87	1.25	0.56	0.03	
2015.20	1.25	0.05	0.02	
2034.79	1.25	0.08	0.02	
2051.27	1.25	0.35	0.02	
2061.51	1.25	0.96	0.10	
2073.10	1.25	0.15	0.05	
2078.32	1.30	0.36	0.04	
2116.56	1.30	1.45	0.20	
2147.65	1.30	1.50	0.30	
2162.76	1.30	1.80	0.20	
2178.03	1.30	1.50	0.20	
2196.29	1.35	1.10	0.20	
2216.2	1.40	0.25	0.05	
2221.95	1.40	1.40	0.20	
2270.18	1.45	0.20	0.05	
2276.13	1.45	0.85	0.20	
2286.60	1.50	4.60	0.40	
2321.52	1.50	0.12	0.10	
2335.41	1.55	1.80	0.30	
2352.55	1.55	0.60	0.15	
2362.6	1.60	0.10	0.05	
2374.6	1.60	1.65	0.30	
2381.6	1.60	0.15	0.05	
2389.60	1.60	0.04	0.02	
2418.12	1.65	1.40	0.20	
2439.4	1.65	0.10	0.05	
2456.11	1.65	2.90	0.40	
2491.59	1.70	0.04	0.01	
2508.75	1.70	5.00	0.40	
2526.09	1.70	1.00	0.30	
2563.10	1.75	4.00	0.50	
2568.45	1.75	1.00		
2611.89	1.75	1.15	0.20	
2622.9	1.80	0.10	0.05	
2634.02	1.80	2.50	0.50	
2654.56	1.85	0.06	0.02	
2663.97	1.85	3.00	0.50	
2677.23	1.85	0.20	0.05	
2688.68	1.90	2.80	0.20	
2713.74	1.90	1.150	0.25	
2721.52	1.95	0.12	0.05	
2733.25	1.95	5.80	0.20	
2747.04	2.00	0.15	0.05	
2763.80	2.00	0.06	0.04	
2772.92	2.00	0.98	0.02	
2793.08	2.05	2.25	0.25	
2815.50	2.05	0.40	0.1	
2831.99	2.10	0.50	0.1	
2852.79	2.10	2.75	0.25	
2882.31	2.15	0.24	0.15	
2895.10	2.15	0.25	0.10	
2914.44	2.15	0.16	0.08	
2947.12	2.15	1.40	0.30	
2955.92	2.20	0.58	0.20	
2964.77	2.20	0.38	0.20	
2978.11	2.20	0.20	0.10	
2989.30	2.25	0.60	0.20	
3006.2	2.25	0.15	0.05	
3016.41	2.25	0.43	0.10	
3027.82	2.30	3.15	0.30	
3039.29	2.30	0.70	0.15	
3049.7	2.30	0.18	0.08	
3060.10	2.30	0.55	0.05	
3081.12	2.35	0.85	0.20	
3102.4	2.40	0.05	0.05	
3109.4	2.40	0.60	0.20	
3147.94	2.40	6	2	
3152.79	2.40	6.5	2	
3163.8	2.45	0.32	0.10	
3187.10	2.45	1.25	0.25	
3206.95	2.50	1.8	0.25	
3229.51	2.50	0.20	0.05	
3242.15	2.55	0.20	0.05	
3252.3	2.55	1.10	0.25	
3267.65	2.55	0.60	0.20	
3296.04	2.60	6	1	
3316.92	2.60	0.05	0.05	
3330.08	2.65	1.00	0.20	
3340.65	2.65	2.5	0.25	
3371.4	2.65	0.05	0.03	
3383.48	2.65	1.75	0.25	
3410.66	2.75	0.50	0.10	
3421.63	2.75	0.15	0.10	
3428.6	2.75	0.17	0.10	
3443.72	2.75	0.80	0.20	
3471.63	2.80	0.50	0.20	
3491.37	2.80	0.20	0.06	
3519.87	2.85	1.75	0.25	
3566.2	2.90	0.04	0.04	
3574.99	2.90	0.20	0.10	
3592.66	2.95	0.36	0.10	
3610.47	3.00	1.35	0.25	
3622.41	3.00	0.50	0.20	
3637.42	3.00	0.30	0.10	
3649.50	3.00	1	0.25	
3673.84	3.05	0.32	0.10	
3692.25	3.05	0.50	0.20	
3707.0	3.10	0.48	0.20	
3723.25	3.10	4	1	
3732.62	3.15	1	0.30	
3745	3.15	0.26		
3757.80	3.15	0.30	0.10	
3786.43	3.20	0.40	0.15	
3818.62	3.25	0.28	···	
3825.11	3.25	3.5	1	
3847.95	3.30	0.40	0.20	
3867.68	3.30	0.65	0.10	
3884.25	3.30	0.30	0.10	
3904.27	3.35	4	1	
3931.20	3.40	1.31	0.30	
3961.84	3.40	···		
3968.69	3.40	···		
3975.57	3.40	···		
4000.30	3.45	···		

[a] E_0 and ΔE_0 in eV. Γ_n^0, $\Delta\Gamma_n^0$ and Γ_γ in meV. Γ_n^0 values up to 69.2 eV are from Utley and Jones (Harwell).

TABLE II. Neutron resonance level parameters of U^{238}.

E_0 (eV)	ΔE_0	Γ_n^0 (meV)	$\Delta\Gamma_n^0$	E_0 (eV)	ΔE_0	Γ_n^0 (meV)	$\Delta\Gamma_n^0$	E_0 (eV)	ΔE_0	Γ_n^0 (meV)	$\Delta\Gamma_n^0$
6.68		0.59	0.004	1177.62	0.55	1.85	0.15	2620.6	1.85	0.80	0.40
*10.2[a]		0.0004	0.0002	1194.96	0.55	2.65	0.30	2631.6	1.85	0.02	0.02
21.00		1.90	0.065	1210.93	0.60	0.26	0.05	2672.8	1.90	3.40	1.00
36.70		5.14	0.15	1245.12	0.60	6.50	0.50	2695.6	1.90	0.45	0.10
66.30		3.09	0.12	1267.01	0.60	0.75	0.05	2716.8	1.95	1.36	0.30
80.77		0.23	0.02	1273.20	0.60	0.80	0.05	*2730.0	1.95	0.05	0.05
*90.00	0.15	0.008	0.001	1298.44	0.65	0.08	0.03	2750.1	2.00	0.75	0.25
102.78	0.20	6.50	0.20	1317.21	0.65	0.11	0.02	2761.9	2.00	0.30	0.05
116.93	0.25	3.33	0.14	1335.72	0.65	0.03	0.02	2787.9	2.00	0.20	0.08
145.80	0.25	0.07	0.027	1393.00	0.70	3.70	0.50	*2798.0	2.00	0.05	0.05
165.54	0.30	0.27	0.03	1405.11	0.70	2.05	0.20	3806.2	2.05	0.13	0.05
190.34	0.30	10.90	0.20	*1410.00	0.75	0.03	0.03	2828.6	2.05	0.17	0.05
208.65	0.35	3.90	0.40	*1417.00	0.75	0.03	0.02	*2845.2	2.10	0.05	0.05
237.40	0.10	1.80	0.10	1419.64	0.75	0.25	0.10	2866.1	2.10	1.48	0.10
*242.88	0.10	0.01	0.002	1427.73	0.75	0.80	0.10	2882.9	2.10	9.80	1.00
*263.94	0.10	0.014	0.002	1444.10	0.75	0.57	0.01	2897.8	2.15	0.50	0.25
273.74	0.10	1.52	0.10	1473.80	0.80	2.05	0.20	*2908.5	2.15	0.05	0.05
291.11	0.15	0.90	0.10	1523.10	0.80	5.50	0.50	2923.6	2.15	0.08	0.04
311.12	0.15	0.056	0.004	1532.00	0.80	0.05	0.02	2932.3	2.15	0.46	0.20
347.92	0.20	4.40	0.40	*1546.00	0.85	0.02	0.02	2956.3	2.20	0.28	0.10
376.92	0.20	0.058	0.004	1550.00	0.85	0.03	0.02	2967.4	2.20	0.15	0.05
397.56	0.20	0.30	0.05	1565.00	0.85	0.05	0.01	*2974.0	2.20	0.05	0.05
410.23	0.25	0.95	0.05	1598.16	0.85	8.00	0.50	2987.4	2.25	0.10	0.05
434.19	0.25	0.40	0.07	1622.89	0.90	2.10	0.30	3003.1	2.25	1.70	0.50
*454.17	0.25	0.02	0.005	1638.19	0.90	1.00	0.12	3015.0	2.25	0.13	0.05
463.31	0.30	0.24	0.02	*1645.40	0.90	0.02	0.02	3029.0	2.30	2.50	0.50
478.70	0.30	0.14	0.03	1662.08	0.95	4.00	0.50	3041.0	2.30	0.05	0.02
*488.89	0.30	0.02	0.005	1688.33	0.95	1.90	0.30	3060.2	2.30	0.50	0.10
518.59	0.30	1.90	0.10	*1700.71	0.95	0.02	0.02	3081.1	2.35	0.08	0.03
535.49	0.35	1.60	0.10	1709.40	0.95	1.35	0.15	3109.4	2.40	1.80	0.50
*556.05	0.35	0.02	0.01	1723.00	1.00	0.33	0.04	3133.2	2.40	0.10	0.05
580.20	0.40	1.12	0.03	1744.00	1.00	0.04	0.01	3149.0	2.40	1.10	0.20
595.15	0.20	3.35	0.20	1755.80	1.00	1.50	0.50	3169.0	2.45	0.18	0.02
619.94	0.20	1.14	0.04	1782.30	1.05	11.00	1.00	3179.4	2.45	1.10	0.40
*623.53	0.20	0.017	0.007	1797.70	1.05	0.05	0.02	3189.0	2.45	0.77	0.30
628.67	0.20	0.16	0.02	1808.26	1.05	0.40	0.10	3206.0	2.50	1.00	0.30
661.18	0.25	4.50	0.25	1845.60	1.10	0.31	0.05	3226.0	2.50	0.40	0.10
*677.00	0.25	0.02	0.01	1902.27	1.15	0.48	0.10	3249.2	2.55	0.20	0.05
693.23	0.25	1.30	0.05	1917.10	1.15	0.50	0.05	3280.0	2.55	1.80	0.20
708.46	0.25	0.70	0.10	1968.66	1.20	13.00	1.00	3295.0	2.60	0.15	0.05
721.80	0.25	0.05	0.01	1974.65	1.20	10.50	1.00	3310.9	2.60	1.65	0.20
*730.10	0.25	0.03	0.01	2023.58	1.25	4.50	0.50	3321.3	2.60	1.42	0.20
732.26	0.30	0.05	0.005	2031.06	1.25	1.10	0.10	3334.0	2.65	1.00	0.15
*742.95	0.30	0.02	0.005	2088.63	1.30	0.30	0.05	3355.7	2.65	1.30	0.20
765.05	0.30	0.24	0.04	2096.49	1.30	0.22	0.05	3371.0	2.65	0.05	0.02
779.14	0.30	0.06	0.005	2124.35	1.35	0.10	0.05	3387.8	2.70	0.14	0.04
790.88	0.30	0.18	0.02	2145.95	1.35	0.75	0.10	3409.0	2.70	1.80	0.50
821.58	0.35	2.05	0.10	2152.77	1.35	3.80	0.40	*3419.0	2.75	0.05	0.05
*846.62	0.35	0.02	0.005	2172.00	1.40	0.05	0.03	3436.9	2.75	3.25	0.50
851.02	0.35	1.90	0.10	2185.99	1.40	7.80	0.80	3459.1	2.80	6.50	1.00
856.15	0.35	2.75	0.15	*2194.00	1.40	0.05	0.05	*3470.0	2.80	0.02	0.02
866.52	0.35	0.14	0.02	2201.42	1.40	2.40	0.40	3484.3	2.80	2.00	1.00
*891.29	0.35	0.03	0.01	2229.96	1.45	0.10	0.03	3492.0	2.80	0.19	0.10
905.11	0.35	1.50	0.05	2235.73	1.45	0.10	0.05	3512.0	2.85	0.05	0.02
909.90	0.38	0.03	0.01	*2241.53	1.45	0.03	0.03	3526.0	2.85	0.18	0.10
925.18	0.40	0.28	0.02	2259.06	1.45	1.38	0.15	3561.5	2.90	2.40	0.80
*932.50	0.40	0.01	0.01	2266.43	1.50	3.05	0.20	3574.0	2.90	4.00	1.00
936.87	0.40	4.80	0.50	2281.27	1.50	2.30	0.10	3593.0	2.95	0.26	0.05
958.43	0.40	5.10	0.50	2288.70	1.50	0.05	0.02	*3600.0	2.95	0.05	0.05
991.78	0.45	11.00	0.50	*2302.0	1.50	0.02	0.02	3611.0	2.95	0.05	0.02
1000.30	0.45	0.04	0.04	2315.9	1.50	0.30	0.10	3625.0	3.00	0.05	0.02
1011.25	0.45	0.06	0.02	2337.4	1.55	0.10	0.05	3630.0	3.00	3.60	0.50
1023.00	0.45	0.20	0.04	2352.0	1.55	1.30	0.50	*3647.0	3.00	0.05	0.05
1029.08	0.45	0.10	0.03	2356.0	1.55	1.30	0.50	*3674.0	3.05	0.05	0.05
*1033.16	0.45	0.02	0.02	2392.5	1.60	0.23	0.10	3693.0	3.05	4.00	1.00
1053.93	0.45	2.30	0.50	2410.2	1.60	0.09	0.03	3717.7	3.10	1.00	0.25
1068.10	0.45	0.02	0.02	2426.5	1.65	1.65	0.30	3733.3	3.10	2.50	1.00
*1070.50	0.50	0.01	0.01	2446.2	1.65	2.25	0.25	3764.7	3.15	0.56	0.10
*1081.10	0.50	0.02	0.01	2454.0	1.65	0.05	0.03	3783.7	3.20	4.50	1.00
*1094.80	0.50	0.02	0.01	2489.8	1.70	1.10	0.10	*3799.7	3.20	0.05	0.05
1098.35	0.50	0.45	0.10	2520.7	1.75	0.20	0.10	3832.0	3.25	0.10	0.05
*1102.34	0.50	0.02	0.01	2548.7	1.75	6.80	0.80	3858.1	3.30	5.50	1.00
1108.88	0.50	0.90	0.05	2559.3	1.75	4.30	0.50	3871.3	3.30	4.00	1.50
1131.45	0.50	0.06	0.02	2580.7	1.80	4.80	0.50	3895.0	3.30	0.08	0.05
1140.38	0.55	6.50	0.05	2598.7	1.80	11.00	2.00	3904.4	3.35	3.60	0.06
1167.46	0.55	2.35	0.15	*2604.0	1.80	0.05	0.05				

* Levels which are either p-wave or uncertain. E_0 and ΔE_0 in eV. Γ_n^0 and $\Delta\Gamma_n^0$ in meV. Γ_n^0 value up to $E_n = 208$ eV are previously published.

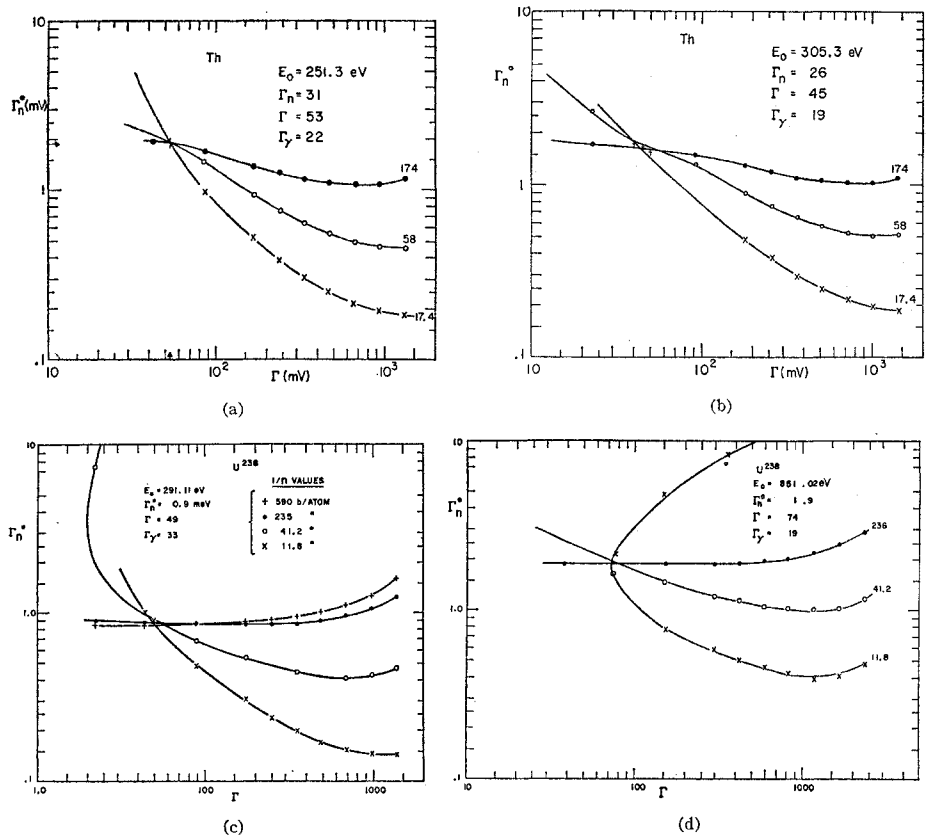

FIG. 3. Some examples of area analysis for obtaining the resonance level parameters for Th and U. The procedure is described in the text.

due to the resonance and interference terms. The area under this curve,

$$A(E_0,E_1,E_2)=\int_{E_1}^{E_2}[1-T'(E)]dE, \qquad (6)$$

is essentially independent of the experimental resolution width if $E_1<E_0$ and $E_2>E_0$ are chosen so $T'(E)$ is ≈ 1 near E_1 and E_2. If the full wing contributions of the resonance to the area are included, either by choosing E_1 and E_2 far enough from E_0, or by adding a correction for the missed wing area, the area is denoted as $A(E_0)$ or A. The contribution of the interference term $\varphi(\beta,x)$ is important for the present measurements.

Values of the ψ and φ have been numerically evaluated as functions of x and β, using electronic computers, by many people using various approximation procedures. Rosen[7] has obtained values of the area function (A/Δ), for a range of values of (Δ/Γ) and $(R/\lambda\!\!\!^{-})^2$, as a function of $(n\sigma_0\Gamma/\Delta)$. His results are given in tabular and graphic form and provide the starting point for our present method of resonance parameter analysis. A program has been developed for use with IBM type 1620 or 7094 computers which provides semiautomatic level analysis for large numbers of resonances by the procedure indicated below.

[7] J. L. Rosen, Columbia Report CU-188 1959 (unpublished).

From preceding programs one obtains cards with the processed experimental data. Each card corresponds to one channel and gives the channel number, the neutron energy, and the T_{exp} and σ_{exp} values for all thickness of a given sample element. This information is studied to establish the resonance positions, etc. The area analysis program is divided into two parts. The first program uses the above "data cards" as input. Cards are also included which specify the resonance channel number for each resonance, the number of channels to be used for each resonance and sample thickness, and T_p for each resonance and sample thickness. The program output gives the $A(E_0,E_1,E_2)/\Delta$ for each resonance and sample thickness, along with other information needed by the second program.

The second program calculates $(n\sigma_0\Gamma/\Delta)$ values for each resonance and sample thickness for a range of choices of (Γ/Δ) using the $A(E_0,E_1,E_2)/\Delta$ values. The wing corrections to the $A(E_0,E_1,E_2)/\Delta$ values are added for each choice of (Γ/Δ) using the known $(1/n)$ and $(R/\lambda\!\!\!^{-})^2$ values. The program uses Rosen's tabulated curves by a procedure that was found to yield suitable accuracy for our purposes. The program uses a standard tabulated curve which, by the use of a set of appropriate stored linear "scale stretching factors," can be made to give a close match to any of Rosen's curves. Interpolation procedures are included to give any curve (of A/Δ versus $n\sigma_0\Gamma/\Delta$) for values of $(R/\lambda\!\!\!^{-})^2$ or $\beta=2\Delta/\Gamma$

intermediate between those for Rosen's tabulated curves.

The calculated values of $g\Gamma_n$ versus Γ from the program output for each resonance are plotted to give one curve for each sample thickness. Usually the intersection position of these curves determines the experimental values for $g\Gamma_n$ and Γ for the resonance. If both $g\Gamma_n$ and Γ are well established, then $\Gamma_\gamma=\Gamma-\Gamma_n$ is also established. In practice there are certain limiting factors which diminish the usefulness of this method. For thick samples the area analysis requires large wing corrections to convert the partial area to a total area. The corrections and the central area are both sensitive to the choice of the effective transmission T_p due to the potential scattering plus the effect of adjacent levels. The intersection point of the Γ_n versus Γ curves is sensitive to the choice of T_p and is somewhat uncertain. The sensitivity to the exact choice of T_p is greatest for the thick samples and strong levels. The thinner samples mainly determine $g\Gamma_n$ for the stronger levels, and the thick samples determine values of $g\Gamma_n$ for very weak levels. These $g\Gamma_n$ values are relatively independent of the assumed value of Γ. In practice the analysis of each level is judged on its own merits as to whether a meaningful value of Γ can be obtained by using "extreme" values of T_p within the region of experimentally plausible values. This is where the complete automation of the analysis ceases to be useful and is of questionable accuracy. The judgment of the experimentalist dominates in the end.

It has been found that, except for the weak levels, the medium thickness and thin samples give the most accurate values for Γ_n, while the thick sample is mainly used to try to determine Γ and thus Γ_γ. Consequently, the error in Γ_γ is usually much larger than that in Γ_n. Moreover, Γ_γ is completely undetermined in many cases.

Examples of the area analysis for some of the favorable cases are shown in Fig. 3. The results for the Γ_n^0 values are given in Table I for Th and Table II for U^{238}. The values of Γ_γ are quoted only when a reasonable estimate of the uncertainty can be made unambiguously. Unfortunately, this is possible only in a few cases. The conditions required to determine Γ_γ include the following: (a) Γ_n must be large, (b) the value of Γ_γ should be comparable to, or larger than Γ_n, and (c) the resonance should be isolated so the contribution of neighboring levels is small and T_p can be evaluated accurately from the wing region.

4. THORIUM RESONANCE PARAMETER RESULTS

The average of the first 10 values of Γ_γ in Table I is 19 meV. (This includes six of our values.) This is in good agreement with the preliminary value of (18.5±1.2) meV obtained by Moxon and Mycock[8] using a capture of γ-ray detector for the measurements. It is in disagreement with the previously favored value[9] $\Gamma_\gamma=(34\pm7)$ meV. The Γ_n^0 values may be determined more precisely if Γ_γ is assumed to be known *a priori*, rather than treated as a second unknown parameter for each level. We have thus used $\Gamma_\gamma=19$ meV in evaluating the Γ_n^0 values for most resonances. The quoted uncertainties in the Γ_n^0 values are chosen in a somewhat arbitrary manner after studying the analysis and the transmission curves for the separate resonances. They are believed to be conservatively large estimates of the over-all uncertainty. The neutron widths up to $E=1300$ eV reported by Utley and Jones[6] are in reasonable agreement with our values for most of the resonances. The resonance parameters for the first four levels listed in Table I are those of Utley and Jones.[6]

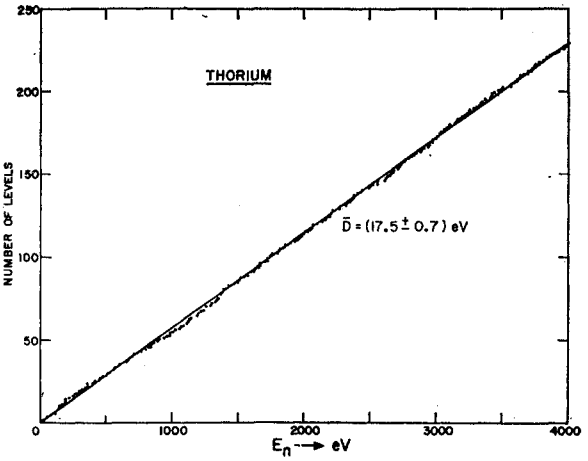

FIG. 4. Plot of the cumulative number of levels observed in Th^{232} versus E_n.

Figure 4 shows a plot of the number of levels observed versus neutron energy. It should be emphasized that a certain judgment factor is involved in deciding for or against the existence of some of the "levels" which might really be weak levels or just be statistical fluctuations in the data which were mistakenly counted as levels. If a level recognition threshold is set too high, weak levels will be missed. If it is set too low, false levels will be included. Two different persons, or the same person at different times, might arrive at slightly different numbers of levels. However, one hopes that the two opposite effects will tend to cancel each other and will provide a close approximation to the correct number of levels. One also hopes that the net effect of such errors will not seriously affect the results for the observed distribution of level spacings and Γ_n^0 values, etc. The level density for $l=0$ resonances should be constant over the region of a few keV so the near constancy of the average density in our measurements

[8] M. C. Moxon and M. C. Mycock, Harwell Progress Report, AERE PR/NP4 (unpublished).

[9] D. J. Hughes, B. A. Magurno, and M. K. Brussel, Brookhaven National Laboratory Report BNL 325, Suppl. 1, 2nd ed., January 1960 (unpublished).

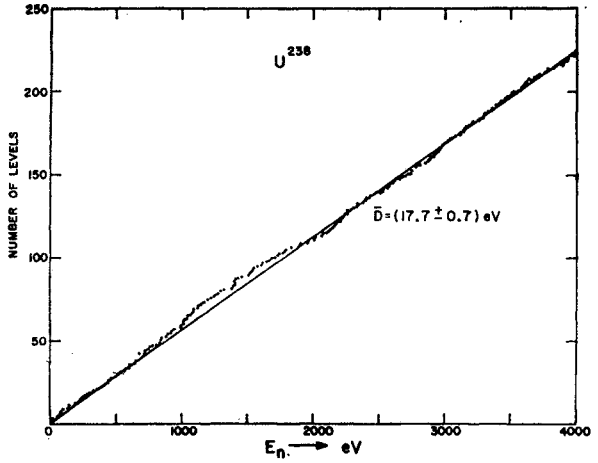

FIG. 5. Plot of the cumulative number of levels observed in U^{238} versus E_n.

indicates that we have not missed many levels up to the maximum energy of 4 keV.

If one divides 223 resonances of Th counted to 3.9 keV by the energy range, a value $\langle D\rangle = 17.5$-eV results. Similar calculations for the energy ranges (0—1) keV, (1—2) keV, (2—3) keV, and (3—3.9) keV give $\langle D\rangle = 17.8$ eV, 17.5 eV, 17.2 eV, and 17.3 eV, respectively. This gives some indication of the uncertainty in the result. If one assumes that a correct count has been made which includes only $l=0$ resonances, and n resonances are obtained ($n \gg 1$), the limited statistical sample size determines the uncertainty in knowing the true $\langle D\rangle$. If the level spacings were completely random, a fractional uncertainty $1/\sqrt{n} \sim 7\%$ is implied. The Wigner surmise for level repulsion leads to a certain short range ordering and reduces the fractional uncertainty to $[(4-\pi)/\pi n]^{1/2} = 0.53/\sqrt{n} \sim 3.6\%$ for $n=224$. A much smaller uncertainty of $<0.3\%$ is predicted when long-range order effects are considered. This is discussed in more detail in Sec. 6 D. Our main problem is probably one of including only $l=0$ resonances and the exclusion of $l=1$ and spurious levels. We choose $\langle D\rangle = (17.5 \pm 0.7)$ eV for $l=0$ levels as our experimental result for Th^{232}.

It should be pointed out that measurements with a sufficiently large factor increase in the statistical accuracy for thick sample transmission values would be expected to reveal large numbers of very weak $l=1$ resonances. The resulting much smaller experimental $\langle D\rangle$ would then have a complicated dependence on the true $\langle D\rangle$ values for the $l=0$ and $l=1$ resonance populations separately.

5. U^{238} RESONANCE PARAMETER RESULTS

The analysis for the resonance parameters for U^{238} were performed in the same manner as for Th. The Γ_γ values obtained treating both Γ_n and Γ_γ as unknown for each resonance were in reasonable agreement with earlier measured values.[1,5,9] Our present Γ_γ values have greater uncertainty than the value $\langle\Gamma_\gamma\rangle = (24.6 \pm 0.8)$ meV of the earlier[1] Columbia measurements. For the determination of Γ_n values we chose $\Gamma_\gamma = 25$ meV. All of the Γ_γ values for the different resonances should be close to this value. Changes in Γ_γ of ± 5 meV have relatively little effect on the best choice Γ_n values for the thinner sample data.

The present results for Γ_n^0 for the U^{238} resonances can be compared with the earlier Columbia 35-m results[1] and with the results of Firk *et al.*[5] for energies to ~ 1 keV. Our present measurements have ~ 5 to 10 times better energy resolution than either of those measurements and are expected to yield more reliable Γ_n^0 values, particularly when two levels are so close together that they were previously incompletely resolved. Values of Γ_n^0 are only given for the present measurements for resonance energies $E > 220$ eV. The three sets of results are in reasonable general agreement, although factors ~ 4 disagreement occur in a number of cases. The present results for each resonance usually agree with one of the previous values, or lie between them. The experimental results obtained for the strength function are quite close in the three cases. This is discussed in more detail later.

The U^{238} level spacing is almost identical to that for Th^{232}, since 60, 57, 58, and 56 levels, respectively, are observed in the first four 1-keV energy intervals. This gives $\langle D\rangle = 17.3$ eV. There is reason to believe that a significant number of these resonances are due to $l=1$ interactions, so this is not the $l=0$ value for $\langle D\rangle$. This matter is discussed in more detail in a later section.

Figure 5 shows a plot of the number of levels observed versus neutron energy.

6. OUTLINE OF THE THEORY OF THE STATISTICAL ASPECTS OF RESONANCE SYSTEMATICS

A. The Strength Function Magnitude for $l=0$ and $l=1$

The extensive literature on this subject is partially listed in the references of our previous papers.[1,2] The essential point is that the strength functions, $\langle\Gamma_n^l\rangle/\langle D_l\rangle$, are expected to exhibit a long-range resonance dependence on nuclear size and neutron energy. An optical-model potential $(V+iW)$ is used for the effective interaction of the incident neutron with the target nucleus. The real part of this potential should be roughly the same as that required by the Mayer-Jensen shell model to produce the experimental features of nuclear shell structure. The imaginary part of this potential is associated with the loss of incident neutron flux via incoherent processes. The observation of peaks in the $l=0$ strength function at mass numbers ~ 55, and ~ 150 is in agreement with shell-model results. There should be equal changes in the nuclear radius between successive major peaks. The $l=1$

strength function should have maxima for nuclear radii about midway between those for the $l=0$ resonances. The above remarks are made assuming spherical nuclear shapes. It is well known, however, that nuclei tend to assume quite large spheroidal distortions when the neutron and/or proton numbers are far from major closed shell values. The magnitude of this distortion increases from one major shell to the next and is quite large in the region of Th^{232} and U^{238}. The effect of the distortion is, roughly speaking, as if the major and minor axes of the distorted shape each contributed their own size resonances. The large splitting of the $A\sim150$ peak for $l=0$ is well known. The region of Th and U might be expected to be near the position of a minimum in the $l=0$ strength function and a maximum in the $l=1$ strength function, for low neutron energies, if the nuclei were spherical. The situation is confused by the large spheroidal distortions, however, and the observed $l=0$ strength functions for Th and U are of normal size (i.e., not extra large or small.) Our only good test for the presence of many $l=1$ resonances in our data is by seeing if there seem to be more weak resonances than expected theoretically for an $l=0$ distribution alone. Our Γ_n^0 distribution for Th^{232} is consistent with only $l=0$ observed levels, but the results suggest that a significant number of our weak U^{238} resonances are $l=1$ levels. This suggests that the U^{238} $l=1$ strength function is significantly larger than for Th. The two nuclear sizes are not very different but differences in the distortion from sphericity may account for the difference. This emphasizes the importance of accumulating large amounts of reliable resonance systematics data for a large sample of nuclear species.

B. The Distribution of Γ_n^0 Values About $\langle\Gamma_n^0\rangle$

Present thinking on this subject is based on the theoretical picture of Porter and Thomas.[10] In the Wigner-Eisenbud R-matrix theory of nuclear reactions, the partial width $\Gamma_{\lambda\alpha}$ for the decay of a compound nucleus resonance state λ via channel α may be expressed in the form

$$\Gamma_{\lambda\alpha}=2P_\alpha\gamma_{\lambda\alpha}^2, \tag{7}$$

where P_α is a barrier penetration factor for channel α and $\gamma_{\lambda\alpha}$ is the integral over the channel surface of a normalized eigenstate of the Hamiltonian subject to special boundary conditions at all channel boundaries. The surmise is that the magnitude of $\gamma_{\lambda\alpha}$ should have a random (Gaussian) distribution about zero, with $\langle\gamma_{\lambda\alpha}^2\rangle$ just that for the ensemble of similar levels. For $l=0$ resonances, use of Γ_n^0 removes the energy dependence of P_α and one expects only the one incident channel to contribute to Γ_n^0. As emphasized by Porter and others, there is the nontrivial conceptual problem of whether or not all $l=0$ resonances should be members of a single population having a common $\langle\Gamma_n^0\rangle$. In addition to J and parity for a compound nucleus state one could imagine that there were other good, or partially good, quantum numbers (other than E_λ) which would further divide the resonances into subsets with different $\langle\Gamma_n^0\rangle$ values. A similar question is involved in the distribution of resonances spacings.

If a Gaussian distribution of the $\gamma_{\lambda n}$ values with a common $\langle\gamma_n^2\rangle$ is assumed, the Porter-Thomas distribution results. Let $x=\Gamma_n^0/\langle\Gamma_n^0\rangle$. Then

$$P(x)dx=\frac{dx}{(2\pi x)^{1/2}}e^{-x/2}. \tag{8}$$

If a process such as capture is considered, where processes involving ν channels are counted together as a partial width, then $\Gamma_{\lambda\alpha}$ is the sum of ν terms of the form $2P_\beta\gamma_{\lambda\beta}^2$. In this case $\sqrt{\Gamma_{\lambda\alpha}}$ may be considered a radius vector in a ν-dimensional space having coordinates $z_\beta=(2P_\beta\gamma_{\lambda\beta}^2)^{1/2}$, where each z_β is normally distributed, each with its own $\langle z_\beta^2\rangle$. Surfaces of equal probability are hyperellipsoids in the ν-dimensional space. For the special case of equal $\langle z_\beta^2\rangle$, the surfaces are hyperspheres, and a χ^2 type function of ν degrees of freedom results for $(\Gamma_{\lambda\alpha})^{1/2}$. If a common variation of the P_β terms can be removed, the corresponding distribution of $x=\Gamma_\alpha^0/\langle\Gamma_\alpha^0\rangle$ is of the form

$$P(x)dx=\frac{\nu x^{(\frac{1}{2}\nu-1)}}{2\Gamma(\frac{1}{2}\nu)}\exp[-\tfrac{1}{2}\nu x]. \tag{9}$$

This function is called a χ^2 distribution function for ν degrees of freedom and has been used as a standard comparison function by many authors to compare with observed distributions in Γ_n^0 values, Γ_γ values and *level spacing* distribution functions. There is no good reason to believe that the level spacings follow a formula of this type. The Γ_n values are expected to satisfy this relation for $\nu=1$ if the formula is applicable at all. The Γ_λ value distribution should follow a curve for a large value of ν since capture gamma-ray transitions to many states of the final nucleus contribute, but probably with quite different $\langle z_\beta^2\rangle$ (in the above discussion). Thus, the best match ν for Γ_γ may be much smaller than the number of capture channels.

C. The Strength Function Uncertainty

If one samples n levels of a given population, the expected mean square uncertainty (variance) in the resulting $\langle\Gamma_n^0\rangle$ from the true value for the ensemble is

$$V\langle\Gamma_n^0\rangle\equiv\langle(\Gamma_n^0)^2\rangle-\langle\Gamma_n^0\rangle^2=(2/n)\langle\Gamma_n^0\rangle^2. \tag{10}$$

For ν degrees of freedom $n\nu$ replaces n in Eq. (10). The strength function defined in Eq. (1) is almost completely unaffected by missing weak $l=0$ resonances or by having a few very weak $l=1$ or spurious levels included. The only dependence on n directly is in the deviation of the *true number* of $l=0$ resonances from

[10] C. E. Porter and R. G. Thomas, Phys. Rev. **104**, 483 (1956).

the ensemble mean number expected for the energy range. According to the theory of Dyson and Mehta, as discussed in the next section, this should have negligible effect for $n \gg 1$. The over-all fractional uncertainty in the strength function is found by combining the above contribution, Eq. (10), with the experimental uncertainty in the individual Γ_n^0 measurements. Unless there are systematic experimental effects tending to make the "measured" Γ_n^0 too large or small, the effect in Eq. (10) dominates in the present measurements. This effect is not properly included in many of the experimentally quoted results for S_0 in the literature. The Columbia 35-m U^{238} value[1] for S_0 was based on the Γ_n^0 values for 55 resonances and was stated as $S_0=(0.95\pm0.15)\times10^{-4}$. On the basis of Eq. (10) alone this would be $S_0=(0.95\pm0.18)\times10^{-4}$. On the basis of $\sim$200 levels, a 10% uncertainty is present. To obtain a 1% uncertainty one needs 20 000 levels with $\ll$1% systematic uncertainty in the experimental Γ_n^0 values.

D. The Level Spacing Distribution

During recent years there has been much interest in the understanding of the ordering of level energies in complex nuclear and atomic spectra. In the last few years a large number of theoretical papers on this subject have been published. An appreciable fraction of this literature reflects an interest in the beautiful mathematical aspects of the subject but is not directly applicable for a comparison with our experimental results. A brief orientation summary of the theoretical developments which are necessary for a comparison with our data analysis is presented below.

The original question was "What is the form of the distribution function for the spacing of adjacent levels about the average spacing $\langle D\rangle$?" The corresponding distribution function is denoted as $P^0(x)$, where $x=D/\langle D\rangle$. At a later stage interest also arose in the more complicated distribution functions $P^k(x)$, for the spacing distribution between two levels having k intermediate levels. Moreover one could also calculate the values of various correlation coefficients C defined as

$$C(x,y)\equiv\frac{\langle x_i y_i\rangle-\langle x_i\rangle\langle y_i\rangle}{[(\langle x_i^2\rangle-\langle x_i\rangle^2)(\langle y_i^2\rangle-\langle y_i\rangle^2)]^{1/2}}. \quad (11)$$

This quantity is positive if x and y fluctuate in the same sense and negative if they vary in opposite senses.

For a random level spacing distribution

$$P^0(x)dx=e^{-x}dx \quad (12a)$$

and

$$P^k(x)dx=(x^k e^{-x}/k!)dx. \quad (12b)$$

The presently favored viewpoint on this matter originated with Wigner[11–13] in 1957, although the development of the mathematical concepts extends far into the past. Wigner distinguished sets of levels belonging to the same ensemble by virtue of the same J and parity. Utilizing the concept of level repulsion, he surmised the formula

$$P_w^0(x)dx=(\pi x/2)\exp[-\pi x^2/4]. \quad (13)$$

This formula has given much better agreement with the previous Columbia results[1] for U^{238} than the random distribution. A series of papers by M. L. Mehta and M. Gaudin, culminated in a paper by Gaudin[14] in which he obtained the exact form of $P^0(x)$ for the distribution of eigenvalues of a real $N\times N$ symmetrical matrix having a random distribution of the matrix elements, as $N\to\infty$. He found that the exact form is not identical to $P_w^0(x)$, but is almost indistinguishable from it. Thus the Wigner formula may be regarded as a very good approximation to the exact function.

Much of the present terminology in this field results from a series of papers by F. J. Dyson alone, and in collaboration with Mehta.[15] Dyson shows that there are two ways of selecting the range of the eigenvalues corresponding to a Gaussian ensemble (the previous standard form), and to a circular ensemble (which he introduced). He also introduced a "threefold way" of choosing the type of $N\times N$ matrices corresponding to the "orthogonal group," the "unitary group," or the "symplectic group." All studies using real symmetric Hamiltonian matrices correspond to the orthogonal ensemble which, as pointed out in V, p. 719,[15] is the only ensemble relevant to slow neutron resonances for heavy nuclei. The unitary ensemble lacks time reversal invariance. The symplectic ensemble applies only to odd spin systems without rotational symmetry. The function $P^0(x)$ obtained by Gaudin applies to the orthogonal ensemble. Dyson[15] points out, TFW, p. 1199, that the three ensembles relate to the classical theorem of Frobenius: "Over the real number field there exist precisely three associative division algebras, namely the real numbers, the complex numbers, and the real quaternions." He associates orthogonal, unitary, and symplectic with real numbers, complex numbers, and quaternions, respectively. These have, respectively, $\beta=1$, 2, and 4 components. This $\beta=1$, 2, 4 shows up in Dyson's theory.

Let $E_1, E_2, \cdots E_n$ be the matrix (energy) eigenvalues, and $Q_{n\beta}(E_1,\cdots,E_n)\,dE_1\cdots dE_n$ be the simultaneous probability that E_1 is between E_1 and $E_1+dE_1,\cdots$, and E_n is between E_n and E_n+dE_n. Then one tends to

[11] E. P. Wigner, Canadian Mathematical Congress Proceedings, 1957, p. 174 (unpublished).

[12] E. P. Wigner, Oak Ridge National Laboratory Report No. 2309 1956, p. 59 (unpublished).

[13] E. P. Wigner, Columbia University Report CU-175, T.I.D.-7547, 1957, p. 49 (unpublished).

[14] M. Gaudin, Nucl. Phys. **25**, 447 (1961). References to the earlier literature are given in this paper.

[15] F. J. Dyson, J. Math. Phys. **3**, 140, 157, 166, 1199 (1962), denoted I, II, III, and TFW, and M. L. Mehta and F. J. Dyson, J. Math. Phys. **4**, 701, 713 (1963), denoted IV and V.

obtain

$$Q_{n\beta}(E_1,\cdots E_n)=\text{const}\prod_{i<j}|E_j-E_i|^{\beta}, \quad (14a)$$

where $\beta=1$, 2 or 4. This would favor a blowup of the whole spacing distribution, so some trick is needed to establish the observed average level density. In the usual Gaussian ensemble,[15] TFW, p. 1215, the holding together is obtained by the appearance of an additional Gaussian factor to give

$$Q_{n\beta}(E_1,\cdots,E_n)=\text{const}[\prod_{i<j}|E_i-E_j|^{\beta}]\times\exp[-\sum_j E_j^2/4a^2]. \quad (14b)$$

Since nuclear level densities for high excitation tend to have a roughly exponential increase with nuclear excitation energy, the entire treatment is limited to an energy range sufficiently small that the gross energy dependence of the level density is small. This region should also contain a very large number, N, of levels, of which the experimental sample, n, is a small portion so $N\gg n\gg 1$.

The end effect difficulty in Eq. (14a) is avoided in Dyson's circular ensemble by considering N points, θ_j situated on the unit circle. Then the average point spacing is $2\pi/N$, which corresponds to the actual $\langle D\rangle$, and $|E_i-E_j|$ becomes $|e^{i\theta_i}-e^{i\theta_j}|$. The joint probability distribution function for this case is

$$Q_{N\beta}(\theta_1,\theta_2,\cdots\theta_n)=C_{N\beta}\prod_{i<j}|e^{i\theta_i}-e^{i\theta_j}|^{\beta}. \quad (14c)$$

Mehta and Dyson[15] show, V, p. 714, that $P^0(x)$ for $\beta=4$ is identical with $P^1(x)$ for $\beta=1$, if $x=D/2\langle D\rangle$ for $\beta=1$.

Similarly, Gunson[16] has shown that $P^0(x)$ for $\beta=2$ is identical with $P^0(x)$ for $\beta=1$ for the situation where two $\beta=1$ (noninteracting) populations are present with the same $\langle D\rangle$ for each population, and one counts only every other level to obtain the D and $\langle D\rangle$ for the new $\beta=1$ case.

Following Wigner's surmise, and excluding the papers of Mehta, Gaudin, and Dyson, the main continuing theoretical developments in this field are due to Porter and Rosenzweig. They have studied the properties of finite $N\times N$ real symmetric matrices, with randomly distributed matrix elements. This is the Gaussian orthogonal ($\beta=1$) ensemble. In a number of papers[17–21] they have established the basic theoretical framework of the subject, and have obtained analytic and Monte Carlo results for the various spacing distributions and correlation coefficients, emphasizing detailed comparisons with experimental results. It was shown that the form of $P^0(x)$ is relatively independent of N for $N\geqslant 2$. For $P^1(x)$ one needs $N\geqslant 3$. Porter[20] has obtained an explicit formula for the case $N=3$ using the Gaussian orthogonal ensemble. If $x\equiv D/\langle D\rangle$ and ϕ is the error function, then

$$P_3{}^1(x)=(729/64\pi^2)x\exp(-27x^2/16\pi)\times\{[x^2-(8\pi/9)]\phi(3x/4\pi^{1/2})+(\tfrac{4}{3}x)\exp(-9x^2/16\pi)\}. \quad (15)$$

This has the asymptotic forms for large and small x:

$$P_3{}^1(x)\underset{x\to 0}{\longrightarrow}(729/64\pi^3)x^4, \quad (16a)$$

$$P_3{}^1(x)\underset{x\to\infty}{\longrightarrow}(729/64\pi^2)x^3\exp(-27x^2/16\pi). \quad (16b)$$

He also obtained a value of -0.253 for the correlation coefficient between adjacent level spacings [i.e., where $D_i\to x_i$ and $D_{i+1}\to y_i$ in Eq. (11)].

Kahn[22] has computed the form of $P^1(x)$ using the circular orthogonal ensemble as $N\to\infty$ and obtains results in good agreement with Porter's results for $N=3$. He has also calculated $P^0(x)$ for $\beta=2$ as $N\to\infty$. The result is in close agreement with the explicit form $P_2{}^0(x)$ for $N=2$, $\beta=2$, where

$$P_2{}^0(x)=(32x^2/\pi^2)\exp[-4x^2/\pi]. \quad (17)$$

Various calculations using $N\times N$ matrices tend to show that *all* results are relatively insensitive to the dimension N of the matrices involved.

Monte Carlo calculations have been carried out by Porter and others using 10×10 and 20×20 real symmetrical random matrices (Gaussian orthogonal). Histograms of higher order spacing terms $P^k(x)$, and approximate evaluations of various correlation coefficients can be obtained from these results. These results have been used by Garrison[23] for a comparison with our preliminary data on Th.

Dyson and Mehta, IV,[15] emphasize the long-range aspects of the spacing distribution by examining the expected form for a step plot of $N(E)$ versus E. Suppose that n levels are found in an energy region of width $2L$, and that the center of the interval is chosen as a new origin. Among others, they treat the observed number of levels, n, and the quantity

$$\Delta\equiv{}_{A,B}{}^{\text{Min}}\left\{\frac{1}{2L}\int_{-L}^{L}[N(E)-AE-B]^2dE\right\}. \quad (18)$$

[16] J. Gunson, J. Math. Phys. **3**, 752 (1962).
[17] C. E. Porter and N. Rosenzweig, Ann. Acad. Sci. Fennicae Ser. A VI, No. 44 (1960). This contains a lengthy bibliography of earlier papers.
[18] N. Rosenzweig and C. E. Porter, Phys. Rev. **120**, 1698 (1960).
[19] N. Rosenzweig and C. E. Porter, Phys. Rev. **123**, 853 (1961).
[20] C. E. Porter, Nucl. Phys. **40**, 167 (1963).
[21] C. E. Porter, Phys. Today, Vol. 16, No. 2 (1963).
[22] P. B. Kahn, Nucl. Phys. **41**, 159 (1943).
[23] J. D. Garrison, in Proceedings of the Symposium on Statistical Properties of Atomic and Nuclear Spectra, 3 May 1963 (unpublished). The proceedings present a number of invited papers covering recent aspects of the experimental and theoretical work in this area. Copies may be obtained from Peter B. Kahn, Department of Physics, State University of New York at Stony Brook, Stony Brook, New York.

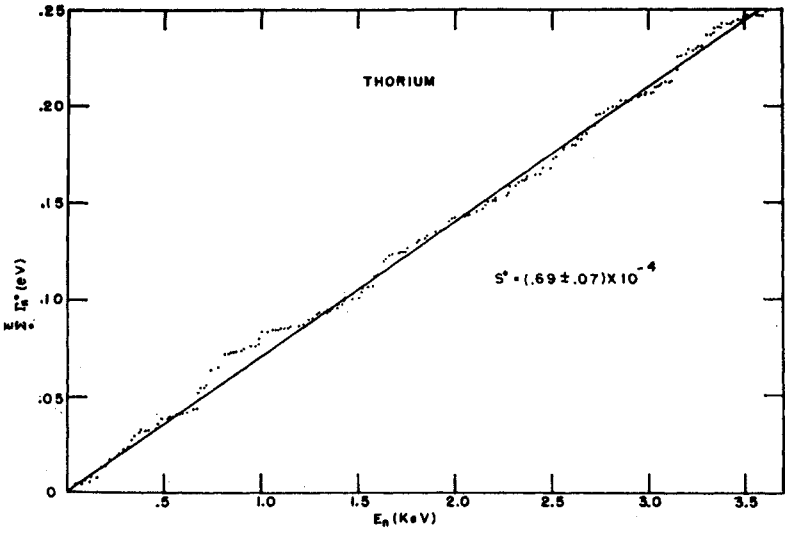

FIG. 6. Plot of $\Sigma(\Gamma_n^0)$ versus E for Th^{232}. The slope of the curve determines the $l=0$ strength function S_0.

Δ is the mean-square deviation between the experimental step function and the best match straight line. They find for the expected averages and variances of n and Δ, for $n \gg 1$,

$$\langle n \rangle = n, \tag{19a}$$

$$V_n = 0.2026[2.181 + \ln n], \tag{19b}$$

$$\langle \Delta \rangle = (1/\pi^2)[\ln n - 0.0687], \tag{20a}$$

$$V_\Delta = 1.1690/\pi^4. \tag{20b}$$

These remarkable results suggest an almost crystal structure long-range behavior for the level positions, with $|(N(E) - AE - B)| < 1$ for most of the interval. The results are extremely sensitive to a very few extra, or missed levels for the ensemble. It is difficult to obtain experimental results sufficiently free from such effects that meaningful comparisons with these formulas can be made at this time. We thus mainly emphasize shorter range phenomena using analyses designed to take account of the limitations of the experimental results.

Certain results for the spacing distribution function $P_\beta^k(x)$ for small x are easily seen from the general form of Eq. (14a, b, c). For $P_\beta^0(x)$ as one spacing $\to 0$, and the other spacings remain essentially constant, the particular x^β dominates the dependence on x for small x. For $P_\beta^1(x)$ let y, $(x-y)$, and x be three spacings 1–2, 2–3, and 1–3. For a given x the value of y can vary as $0 \leqslant y \leqslant x$, giving an integral of the form ${}_0\int^x x^\beta (x-y)^\beta y^\beta dy$ which varies as $x^{3\beta+1}$. Similarly $P_\beta^k(x)$ involves $[1+2+\cdots+(k+1)]$ spacings and k variables dy_1, dy_2, dy_3, $\cdots$, dy_k for the intermediate levels. This gives an x^m form for small x, where $m = [\beta(k+1)(k+2)/2 + k]$. The negative value for the correlation coefficient C_0 between adjacent level spacings is readily understood as follows. If levels 1 and 2 are close together, level 1 also repels level 3 stronger for a given 2–3 spacing than if the 1–2 spacing were larger.

7. RESULTS FOR THE $l=0$ STRENGTH FUNCTIONS

Figures 6 and 7 show plots of $\sum \Gamma_n^0$ versus energy for Th^{232} and U^{238}, respectively. From Eq. (1) the average slopes give the $l=0$ strength functions (S_0). The best choice values are taken to be

$$S_0 = (0.69 \pm 0.07) \times 10^{-4} (Th^{232}),$$
$$S_0 = (0.90 \pm 0.10) \times 10^{-4} (U^{238}).$$

The expected fractional rms uncertainty [Eq. (10)] is $(2/n)^{1/2}$ which is about 10% for $n \sim 200$ in each case. Table III shows the results of S_0 for Th^{232} and U^{238} in successive intervals of 200 eV, where $n \sim 11$ for each interval. Thus a rms variation of about 43% from the mean value is expected. For Th^{232} this corresponds to $\pm 0.30 \times 10^{-4}$ and for U^{238} this is $\pm 0.39 \times 10^{-4}$. The deviation of the observed values of S_0 exceeds the corresponding values for 5 of the 19 intervals for the case of Th^{232} and for 8 of the 20 intervals in the case of U^{238}.

Our choice of $S_0 = 0.90 \times 10^{-4}$ for U^{238} gives less weight to the 3–4-keV energy interval where the deviation of S_0 from the mean value is greatest, but the analysis of resonance parameters is also least reliable in this region. For 1-keV energy intervals a value of $\sim 19\%$ rms spread about the mean value is expected. This corresponds to values of ± 0.13 and $\pm 0.17 \times 10^{-4}$, respectively, for Th^{232} and U^{238}. The observed deviation from the mean for S_0 is this large only for the 3–4-keV energy interval for U^{238}. This suggests that the lower value of S_0 in this energy interval could be a true statistical fluctuation.

The present results for S_0 for Th^{232} and U^{238} may be compared with previously published results. However, since these values, obtained from the study of individual resonance parameters, are for particular regions of our full energy range, it is more appropriate to compare these results with our results obtained from the common energy interval. The Columbia 35-m result

TABLE III. The strength function, S_0, for Th^{232} and U^{238} in steps of 200 eV, 1000 eV, and the cumulative results. The deviations from the favored final result values are also indicated.

Energy range (eV)	Th^{232} $S_0\times10^4$	Th^{232} $S_0\times10^4-0.69$	U^{238} $S_0\times10^4$	U^{238} $S_0\times10^4-0.90$
0–200	0.81	0.12	1.60	0.70
200–400	0.86	0.17	0.65	−0.25
400–600	0.43	−0.26	0.49	−0.41
600–800	1.17	0.48	0.42	−0.48
800–1000	0.72	0.03	1.48	0.58
0–1000	0.80	0.11	0.93	0.03
1000–1200	0.40	−0.29	0.88	−0.02
1200–1400	0.55	−0.14	0.56	−0.34
1400–1600	0.69	0.00	0.98	0.08
1600–1800	0.76	0.07	1.16	0.26
1800–2000	0.74	0.05	1.26	0.36
1000–2000	0.63	−0.06	0.98	0.08
2000–2200	0.49	−0.20	0.93	0.03
2200–2400	0.59	−0.10	0.63	0.27
2400–2600	0.77	0.08	1.61	0.71
2600–2800	1.01	0.32	0.37	−0.53
2800–3000	0.37	−0.32	0.66	−0.24
2000–3000	0.65	−0.04	0.84	−0.06
3000–3200	1.03	0.34	0.47	−0.43
3200–3400	0.77	0.08	0.46	−0.44
3400–3600	0.23	−0.46	0.99	0.09
3600–3800	0.52	−0.17	0.77	−0.13
3800–4000	···	···	1.05	0.15
3000–3950 or 4000	0.65	−0.04	0.77	−0.13
0–2000	0.71	0.02	0.955	0.05
0–3000	0.69	0.00	0.91	0.01
0–3950	0.69	0.00	···	···
0–4000	···	···	0.88	−0.02

for U^{238} was $S_0=0.95\times10^{-4}$ in the 0–1-keV energy interval. This agrees very well with our present value of 0.93×10^{-4} for the same energy interval. Firk *et al.*[5] obtained a value of $S_0=1.00\times10^{-4}$ from the investigation of 100 levels up to an energy of 1800 eV. This is to be compared with our present value of 0.955×10^{-4} for the 0–2-keV energy interval.

Utley and Jones[6] have measured the Γ_n^0 values for individual Th^{232} resonances up to a neutron energy of 1300 eV. Our present values are in good agreement with theirs in the common energy interval.

Hughes and Pilcher[24] have obtained values of S_0 of $(0.9\pm0.2)\times10^{-4}$ and $(1.1\pm0.2)\times10^{-4}$ for Th^{232} and U^{238}, respectively, from the measurements of the average total cross sections in the keV energy region. These values are systematically higher than our present results by (0.2×10^{-4}). However, in the two measurements, different statistical level samples are involved. Furthermore, any systematic errors which might be present would be different for these two different types of measurements, one involving average cross-section measurements and the other detailed evaluation of individual resonance parameters. In any case their values agree with our present values within the uncertainty of the measurements. If our errors in evaluating Γ_n^0 values are purely random, the contribution of these uncertainties to the quoted S_0 values will be about $\pm0.01\times10^{-4}$ for both Th^{232} and U^{238}. This uncertainty is much smaller than the statistical uncertainty associated with the finite number of samples.

[24] D. J. Hughes and V. E. Pilcher, Phys. Rev. **100**, 1249 (A) (1955).

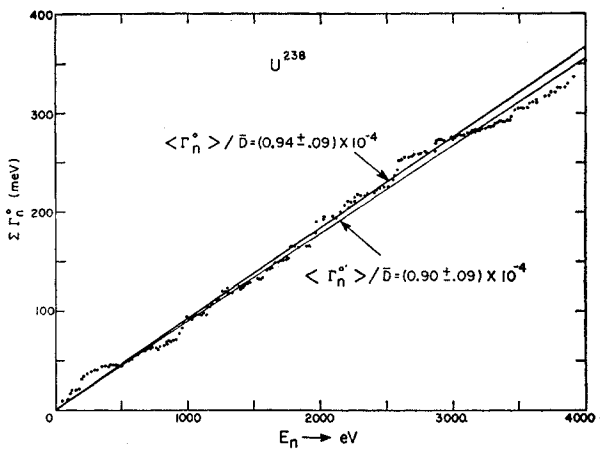

FIG. 7. Plot of $\Gamma_n\Sigma(^0)$ versus E, for U^{238}. The slope of the curve determines the $l=0$ strength function S_0. Two slopes are drawn showing two different possible choices of S_0.

8. THE EXPERIMENTAL DISTRIBUTION OF Γ_n^0 VALUES

Figure 8 shows the distribution function for values of $y=(\Gamma_n^0/\langle\Gamma_n^0\rangle)^{1/2}$ for 171 levels in Th^{232} to 3 keV. The histogram is taken in intervals of $\Delta y=0.2$, where

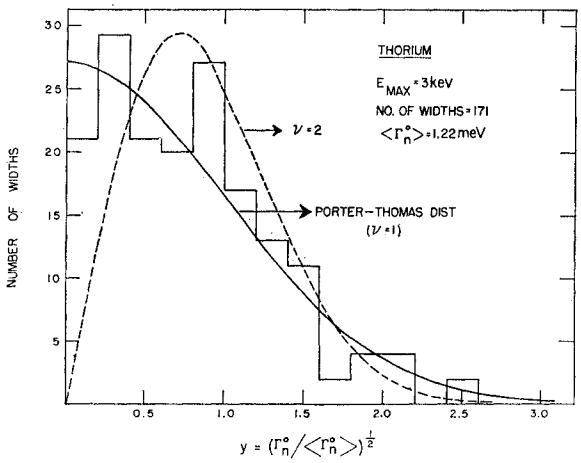

FIG. 8. Histogram plot of the observed experimental distribution of $y=[\Gamma_n^0/\langle\Gamma_n^0\rangle]_j^{1/2}$ for Th^{232}. The Porter-Thomas ($\nu=1$) and the $\nu=2$ theoretical distributions are shown for comparison. The $\nu=2$ curve corresponds to an exponential distribution of Γ_n^0 values.

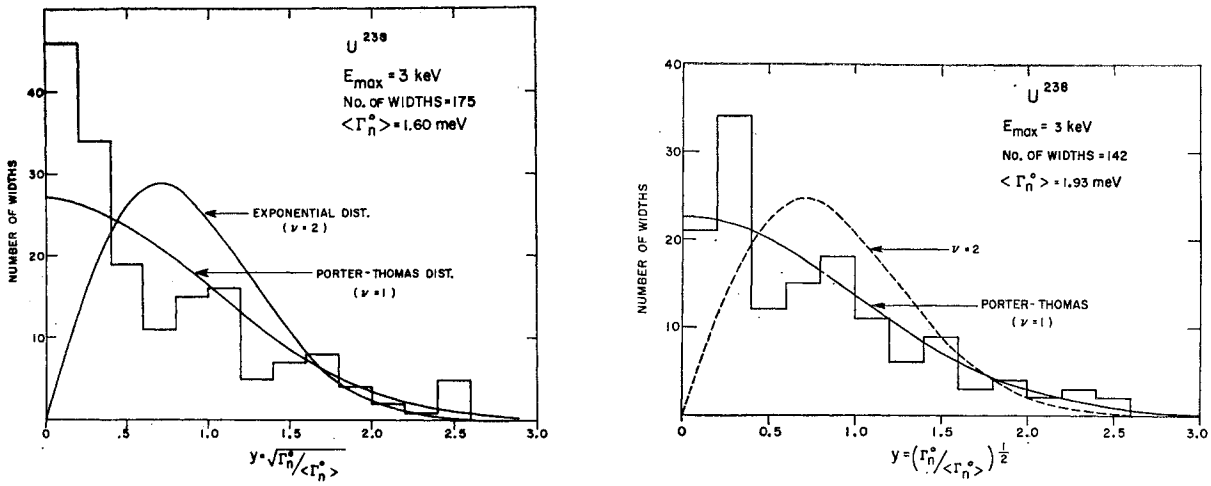

(a) (b)

FIG. 9. (a) Histogram plot of the observed experimental distribution of $y=[\Gamma_n^0/\langle\Gamma_n^0\rangle]_j^{1/2}$ for U^{238}. All of the 175 observed resonances to 3 keV are included. The Porter-Thomas ($\nu=1$) and the $\nu=2$ theoretical distributions are shown for comparison. The experimental data show an excess of small widths. (b) This figure for U^{238} is the same as (a) except that the 33 levels to 3 keV indicated by asterisks in Table II were omitted. Most of the omitted levels are believed to be $l=1$ or spurious levels.

$\langle\Gamma_n^0\rangle=1.22$ meV. The Porter-Thomas distribution [Eq. (8)] corresponds to $\nu=1$ in Eq. (9), while the two-channel $\nu=2$ shape corresponds to an exponential distribution for Γ_n^0. These theoretical functions are also shown in the figure. The Porter-Thomas distribution is Gaussian when plotted against $y=x^{1/2}$ and this is seen to give a better fit than the $\nu=2$ distribution with the experimental data for very small and large values of y. Failure to observe all $l=0$ weak levels would tend to lower the experimental histogram for small values of y and would also overestimate the value of $\langle\Gamma_n^0\rangle$, whereas inclusion of some spurious or $l=1$ levels would produce the opposite effects.

In order to obtain a more quantitative comparison of the experimental results with the theoretical distributions, we have analyzed the experimental data in two ways to determine the best fitting value of ν. The results of the analysis for Th^{232} are shown in Table IV. Since the experimental accuracy of analysis decreases with increasing neutron energy, the upper energy $E_{\max}$ was varied in intervals of 500 eV in order to see how the results of the analysis depend on the choice of $E_{\max}$. The two methods of analysis are sensitive in different ways to possible shortcomings in the experimental results.

TABLE IV. Analysis for the effective member of degrees of freedom, ν, in the Γ_n^0 distribution for Th^{232}.

Energy interval (eV)	No. of levels	Mean $\langle\Gamma_n^0\rangle$ (meV)	ν^a	$\frac{1}{n}\sum\log\frac{\Gamma_n^0}{\langle\Gamma_n^0\rangle}$	$\nu^b+\Delta\nu$
0–500	28	1.41	2.22	−1.04	1.19±0.26
0–1000	56	1.43	1.18	−1.16	1.09±0.19
0–1500	84	1.21	1.07	−1.27	1.00±0.14
0–2000	113	1.26	1.16	−1.04	1.19±0.12
0–2500	142	1.19	1.17	−0.97	1.26±0.12
0–3000	171	1.21	1.23	−0.92	1.31±0.11
0–3500	202	1.22	1.18	−0.89	1.35±0.11
0–3900	223	1.20	1.19	−0.88	1.36±0.10

The parameter ν^a is based on the expected dependence of the variance of x on ν in Eq. (9).

$$\nu^a\equiv\frac{2\langle\Gamma_n^0\rangle^2}{\langle(\Gamma_n^0)^2\rangle-\langle\Gamma_n^0\rangle^2}. \tag{21}$$

This method of analysis has been suggested recently by Wilets.[25] One notes that ν^a depends mainly on the results for the *strong* levels, together with the total level count. The effect of missing true weak resonances or including spurious or $l=1$ weak resonances is almost entirely limited to its effect on the level count. An increase in n causes a decrease in ν^a. The observed n per 500-eV interval is nearly constant, with a slight increase at higher energy. The high value of ν^a in the (0–500)-eV region for Th^{232} is associated with the relative absence of many strong resonances in this region.

The parameter ν^b is based on a maximum likelihood method as suggested by Porter and Thomas.[10] The analysis uses their Eq. (2)

$$\frac{1}{m}\sum_{i=1}^{m}\ln\left(\frac{\Gamma_n^0}{\langle\Gamma_n^0\rangle}\right)_i=F(\nu), \tag{22}$$

where $F(\nu)$ versus ν is plotted in their Fig. 2 for $x_{1/2}=0$. They also give the relation for the uncertainty in ν due to the statistical effects associated with the finite number of levels m of the experimental sample. This method of analysis for ν is found to be particularly

[25] L. Wilets, Phys. Rev. Letters, 9, 430 (1962).

TABLE V. Analysis for the effective number of degrees of freedom ν in the Γ_n^0 distribution for U^{238}.

Energy interval (eV)	No. of levels	Mean spacing $\bar{D}$(eV)	Mean $\langle\Gamma_n^0\rangle$ (meV)	$\nu^{(a)}$	$\frac{1}{n}\sum \ln\Gamma_n^0/\langle\Gamma_n^0\rangle$	(b) $\nu+\Delta\nu$
0– 500	28	17.8	1.67	0.89	−1.73	0.77±0.17
1000	60	16.7	1.55	0.84	−1.70	0.79±0.13
1500	93	16.1	1.38	0.80	−1.72	0.78±0.11
2000	117	17.1	1.60	0.75	−1.61	0.82±0.11
2500	146	17.1	1.55	0.77	−1.57	0.84±0.10
3000	175	17.1	1.57	0.74	−1.55	0.85±0.09
3500	205	17.1	1.50	0.76	−1.49	0.88±0.08
3900	227	17.2	1.52	0.81	−1.47	0.89±0.07
Analysis excluding starred levels						
0– 500	23	21.7	2.11	1.32	−0.92	1.30±0.32
1000	46	21.7	2.01	1.25	−1.00	1.23±0.18
1500	72	20.8	1.78	1.17	−1.13	1.11±0.14
2000	93	21.5	2.00	1.03	−1.10	1.13±0.12
2500	119	21.0	1.90	1.02	−1.11	1.11±0.12
3000	142	21.2	1.93	0.99	−1.11	1.11±0.11
3500	170	20.6	1.81	0.98	−1.12	1.10±0.11
3900	188	20.8	1.83	1.05	−1.10	1.13±0.10

sensitive to obtaining very accurate Γ_n^0 values for the very weak resonances because of the $\ln(\Gamma_n^0)_i$ term. The rise in the value of ν^b in the second half of Table IV correlates with the scarcity of Γ_n^0 values smaller than 0.1 meV in the energy region above 2 keV (see Table I). We believe that this is due to an experimental effect associated with the level analysis. A quoted value of $\Gamma_n^0=(0.05\pm0.05)$ meV in Table II implies that there is some uncertainty as to the existence of the resonance considered. If, however, the level is real its Γ_n^0 value lies between zero and 0.10 meV. The true Γ_n^0 is probably nearer the lower energy end of the range. For $E<1500$ eV a better evaluation of Γ_n^0 for weak resonances is possible and it is encouraging to note the excellent agreement with the *a priori* expected value $\nu=1$ for this portion of the data for Th^{232}. Thus our conclusion is that the distribution of Γ_n^0 for the case of Th^{232} is probably consistent with $\nu=1$.

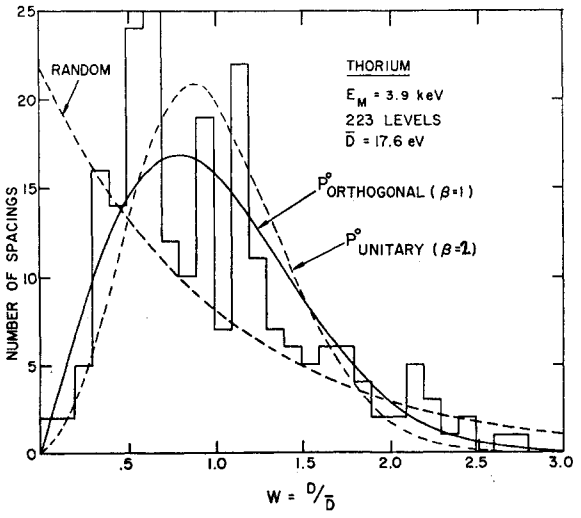

FIG. 10. Histogram of the observed distribution of nearest-neighbor level spacings $x=D/\langle D\rangle$ for Th. The three theoretical curves correspond respectively to random, orthogonal, $(\beta=1)$ and unitary $(\beta=2)$. The orthogonal $(\beta=1)$ curve is the favored theoretical distribution.

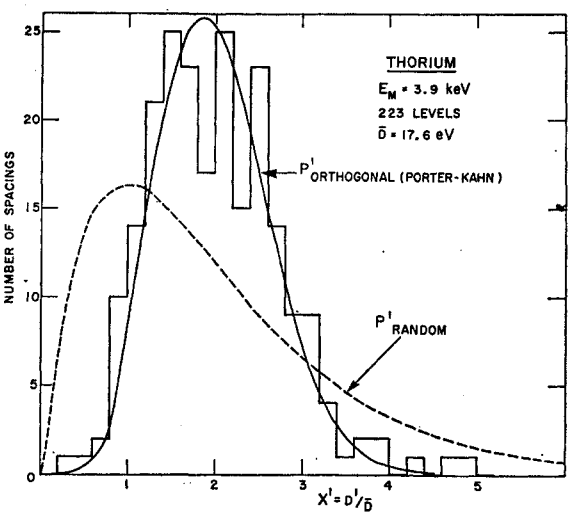

FIG. 11. Histogram of the observed distribution of next-nearest-neighbor level spacings $x=D^1/\langle D\rangle$ for Th^{232}. The theoretical curves for the random and orthogonal (Porter-Kahn) cases are shown. The Porter-Kahn curve is the favored theoretical distribution.

Figures 9(a) and 9(b) show the distribution functions for $y=(\Gamma_n^0/\langle\Gamma_n^0\rangle)^{1/2}$ for U^{238}. As previously discussed,[1] there is reason to believe that the sample includes a number of $l=1$ levels which contribute to the low Γ_n^0 end of the histogram and produce a poor fit to the Porter-Thomas distribution. The levels in Table II indicated by asterisks are considered to be the most likely candidates for spurious or $l=1$ resonances partly on the basis of their small Γ_n^0 values. However, a more severe test is the observed effect of the inclusion or exclusion of any of these levels on the correlation coefficient for adjacent level spacings (as discussed later). Figure 9(a) includes all 175 resonances to 3 keV, while Fig. 9(b) is for the 142 resonances remaining after excluding the 33 starred levels in this interval.

Table V for U^{238} is equivalent to Table IV for Th^{232}. The upper half of the table is based on all levels, while the lower half gives the results obtained by excluding the starred levels. For the second half, both ν^a and ν^b are consistent with $\nu=1$, while ν values systematically lower than one are obtained in the first part where all levels are included in the analysis. This lower value of ν is, however, not due to the experimental bias as this effect will give larger values of ν than the true one. Hence the obvious conclusion seems to be that at least some of the observed levels belong to $l=1$ or are spurious levels.

9. THE LEVEL SPACING DISTRIBUTION

In view of the great current theoretical interest in this topic and because our present results for Th^{232}

TABLE VI. Modified χ^2 tests and moments M^k for the Th^{232} nearest-neighbor spacing distribution. The definitions and significance of the numbers are given in the text.

Energy interval (eV)	No. of levels	Mean $\bar{D}$ (eV)	χ^2 value P_2	P_4	P_6	P_0^0	P_u^0	Moments M^K M^1	M^2	M^3	M^4
0–1000	56	17.8	33.5	19.0	18.8	18.0	25.3	1.01	1.38	2.19	3.83
0–2000	113	17.7	59.6	24.2	19.9	21.9	33.8	1.02	1.37	2.21	3.99
0–3000	171	17.6	105.1	43.2	31.9	37.0	52.2	1.03	1.39	2.29	4.28
0–3900	223	17.5	144.3	55.8	35.8	39.9	51.0	1.03	1.38	2.22	4.06
2000–3000	58	17.2	37.0	17.0	11.7	13.4	14.5	1.02	1.35	2.16	3.98
2000–3900	110	17.2	87.4	40.2	26.5	28.8	30.5	1.03	1.35	2.10	3.80
Theory								1.00	1.32	2.11	3.93

and U^{238} provide the best presently available tests of the theories, we have given particular emphasis to this aspect of our data analysis.

Figure 10 shows the experimental histogram of the nearest-neighbor spacing distribution as a function of $x=D/\langle D\rangle$ for 223 levels in Th^{232} to 3.9 keV. Various theoretical distribution functions, the random distribution [Eq. (12a)], the Wigner distribution [$\beta=1$, orthogonal, Eq. (13)], and the corresponding $\beta=2$ unitary distribution are also shown for a visual comparison. It is quite evident that only the Wigner distribution gives a good fit to the experimental data.

The next-nearest-neighbor spacing distribution $P^1(x)$ for Th^{232} is shown in Fig. 11. For a comparison we also show the theoretical distributions corresponding to the random distribution [Eq. (12b)] and the Porter[20,21] Kahn[22] distribution obtained using the orthogonal ensemble of matrices. The Porter-Kahn distribution gives an obviously superior fit with the experimental results. The few observed spacings for $x>4$ are hard to reconcile with their almost zero probability for the Porter-Kahn distribution. These large spacings could, however, be attributed to the missing of a few weak levels, an effect which would identify them as next-next-nearest-neighbor spacings.

The experimental histogram in Fig. 10 for Th^{232} has a peculiar behavior in the region of $x=0.6$ to $x=1.2$, with relative minima between $x=0.8-1.1$. There seems to be a fine structure which might be called a double or (triple) peak structure. This effect persists when results for independent energy regions are plotted. It is difficult, however, from the present theoretical understanding to see how this effect could be anything else than a statistical fluctuation.

Figures 12 and 13 show the corresponding plots for $P^0(x)$ and $P^1(x)$ for U^{238}. All of the 227 levels observed up to 3.9 keV have been included. The fit of the experimental results with the theoretical distribution for the orthogonal ensemble ($\beta=1$) is seen to be rather good. Moreover when the starred levels are excluded from the analysis, the agreement is improved somewhat (see Table VII and IX).

Tables VI to IX present the results of statistical tests of the Th^{232} and U^{238} nearest- and next-nearest-neighbor spacing distributions. The U^{238} tests were first made using all levels, and then again excluding the

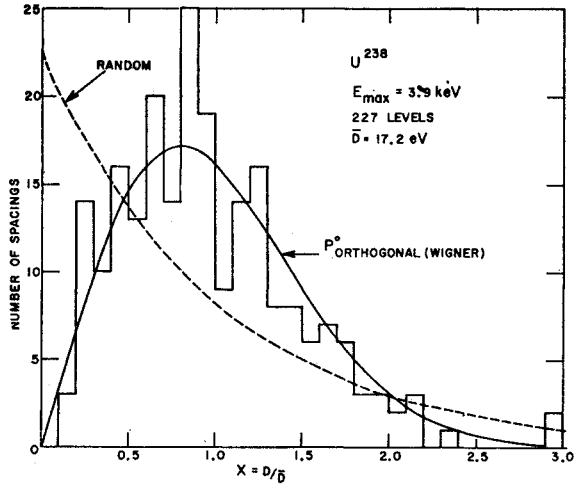

FIG. 12. Histogram of the observed distribution of nearest-neighbor level spacings $x=D/\langle D\rangle$ for U^{238}. The theoretical curves shown for comparison are as explained in Fig. 10.

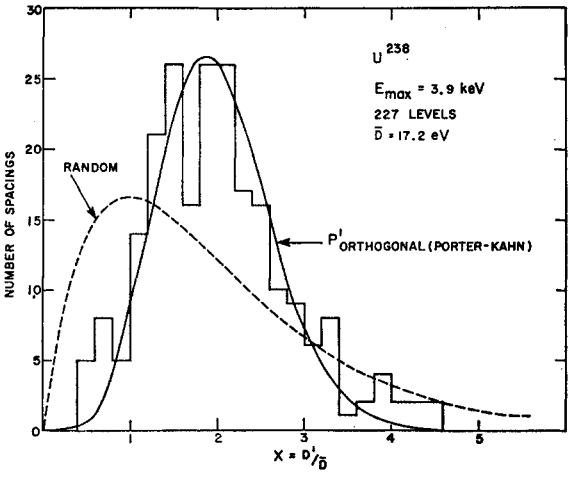

FIG. 13. Histogram of the observed distribution of next-nearest-neighbor level spacings $x=D^1\langle D\rangle$ for U^{238}. The theoretical curves shown for comparison are as explained in Fig. 11.

TABLE VII. Modified χ^2 tests and moments M^k for the Th^{232} next-nearest-neighbor spacing distribution.

Energy interval	No. of levels	$\bar{D}$ (eV)	χ^2 value $P_{\text{Random}}{}^1$	$P_u{}^1$	$P_0{}^1$	Moments M^k M^1	M^2	M^3	M^4
0–1000	56	17.8	26.8	18.2	11.2	2.07	4.91	12.73	35.3
0–2000	113	17.7	37.4	37.6	12.2	2.02	4.79	12.89	38.90
0–3000	171	17.6	68.2	63.8	20.4	2.02	4.72	12.44	36.30
0–3900	223	17.5	102.8	60.1	17.5	2.01	4.64	12.01	34.38
Theory						2.00	4.48	11.09	29.93
2000–3000	58	17.2	24.5	21.1	10.0	2.04	4.78	12.23	34.17
2000–3900	110	17.2	67.7	34.5	19.3	2.03	4.61	11.57	31.52

TABLE VIII. Modified χ^2 tests and moments M^k for the U^{238} nearest-neighbor spacings. All levels are included in the top half of the table while starred levels (see Table II) are excluded in the second half of the table.

Energy interval (eV)	No. of levels	Mean $\bar{D}$ (eV)	χ^2 value P_2	P_4	P_6	$P_0{}^0$	$P_u{}^0$	Moments M^k M^1	M^2	M^3	M^4
0–1000	60	16.7	41.5	21.9	18.2	16.2	21.3	1.04	1.34	1.97	3.14
0–2000	117	17.1	61.0	24.3	19.5	19.5	35.7	0.98	1.27	1.98	3.52
0–3000	175	17.1	94.2	33.7	22.4	24.9	44.7	0.98	1.27	2.00	3.63
0–3900	227	17.2	135.8	46.0	24.3	23.6	33.0	1.00	1.26	1.90	3.27
2000–3000	58	17.2	44.8	23.6	18.2	19.3	22.0	1.00	1.26	1.89	3.23
2000–3900	110	17.2	90.2	40.3	24.7	22.1	25.0	1.03	1.27	1.81	2.89
Analysis excluding starred levels.											
0–1000	46	21.7	39.0	21.7	16.4	14.6	16.0	1.03	1.26	1.73	2.56
0–2000	93	21.5	61.7	26.4	17.3	17.9	19.0	1.03	1.33	2.04	3.61
0–3000	142	21.2	87.5	32.0	17.7	17.2	20.0	1.04	1.36	2.12	3.80
0–3900	188	20.8	131.3	50.5	28.3	29.8	32.0	1.04	1.35	2.10	3.82
2000–3000	49	20.4	35.5	18.8	14.7	14.1	18.0	1.00	1.25	1.76	2.73
2000–3900	95	20.0	75.3	33.5	20.5	18.5	21.0	1.03	1.29	1.93	3.40
Theory								1.00	1.32	2.11	3.93

TABLE IX. Modified χ^2 tests and moments M^k for the U^{238} next-nearest-neighbor spacing distribution. The starred levels were omitted for the second half of the table.

Energy interval (eV)	No. of levels	$\bar{D}$ (eV)	χ^2 values $P_{\text{random}}{}^1$	$P_u{}^1$	$P_0{}^1$	Moments M^K M^1	M^2	M^3	M^4
0–1000	60	16.7	27.6	26.3	15.2	2.03	4.73	12.16	33.58
0–2000	117	17.1	32.4	97.4	45.4	2.03	5.07	14.86	49.79
0–3000	175	17.1	57.30	131.7	56.4	2.02	4.90	13.80	44.30
0–3900	227	17.2	82.9	110.0	36.0	2.02	4.78	12.90	39.50
Analysis excluding starred levels									
Energy interval (eV)	No. of levels	$\bar{D}$ (eV)	χ^2 values $P_R{}^1$	$P_u{}^1$	$P_0{}^1$	Moments M^1	M^2	M^3	M^4
0–1000	46	21.7	34.9	8.0	7.5	2.05	4.54	10.65	26.2
0–2000	93	21.5	50.5	13.8	6.1	2.03	4.61	11.56	31.69
0–3000	142	21.2	86.0	23.3	11.0	2.01	4.48	10.98	29.33
0–3900	188	20.8	116.0	27.3	12.8	2.01	4.50	11.1	30.3
2000–3000	49	20.4	36.3	13.8	11.2	2.06	4.61	11.13	28.69
2000–3900	95	20.0	65.1	17.6	12.7	2.04	4.59	11.41	31.2
Theory						2.00	4.48	11.09	29.93

TABLE X. The parameter correlation coefficients for Th^{232} and U^{238}.

Energy interval (eV)	$[(\Gamma_n^0)_j(\Gamma_n^0)_{j+1}]$ Th^{232}	U^{238}(all)	U^{238}(part)	$[D_jD_{j+1}]$ Th^{232}	U^{238}(all)	U^{238}(part)	$[(\Gamma_n^0)_jD_j]$ Th^{232}	U^{238}(all)	U^{238}(part)
0–1000	−0.04±0.14	0.26±0.12	0.22±0.14	−0.20±0.13	+0.09±0.13	−0.23±0.14	0.23±0.13	0.34±0.12	0.14±0.15
0–2000	−0.01±0.09	0.19±0.09	0.14±0.10	−0.19±0.09	+0.07±0.09	−0.18±0.01	0.13±0.09	0.38±0.08	0.21±0.10
0–3000	−0.07±0.08	0.18±0.07	0.16±0.08	−0.21±0.07	−0.04±0.08	−0.26±0.08	0.13±0.08	0.25±0.07	0.10±0.08
0–3750	−0.03±0.07	0.17±0.07	0.18±0.07	−0.19±0.06	−0.02±0.07	−0.22±0.07	0.12±0.07	0.23±0.06	0.15±0.07
Weighted mean	−0.03±0.07	0.17±0.07	0.17±0.07	−0.21±0.07	−0.03±0.07	−0.24±0.07	0.12±0.07	0.23±0.06	0.15±0.07
Theory	?			−0.25			?		

starred levels (see Table II). Various statistical test procedures are available but we wished to use a form which would emphasize the strengths of the data rather than its weaknesses. The likelihood function provides the most rigorous test, but it would give extreme weightings to the regions of small and large x, where the theoretical function values are very small. The three experimental spacings for $x>4.1$ in Fig. 11 would dominate the result. Since the experimental occurrence of such points is excessively sensitive to a few missed levels, such a test procedure was excluded. The usual χ^2 test of a histogram versus theory is only meaningful when the number of events in each box is large, so a Gaussian is a good approximation for a Poisson distribution. Therefore we have adopted the following arbitrarily modified χ^2 test which gives reduced weight to the regions where the theoretical histogram value f_j is small. If N_j is the experimental histogram value for interval j, then we define χ^2 by

$$\chi^2=\sum_j (N_j-f_j)^2/(f_j+1).$$

In the tables (VI–IX), P_2, P_4, and P_6 are the chi-squared distributions for 2, 4, and 6 degrees of freedoms [Eq. (12b)]. P_0^0 and P_0^1 are the Wigner and Porter-Kahn distributions obtained from the random matrix model using a Gaussian orthogonal ensemble of matrices ($\beta=1$), and P_u^0 and P_u^1 are corresponding ($\beta=2$) unitary ensemble distributions. The functions P_4 and P_6 are not expected to be related theoretically to the true distributions but the chi-squared family of curves have similar general shapes as the P_0 and P_u distributions for appropriate k values. P_2 corresponds to the random distribution for nearest-neighbor spacings. It is seen from Tables VI and VIII that the observed χ^2 values are relatively much smaller for P_6 and P_0 distributions than for other distributions in all cases. It is also evident that the agreement of the U^{238} results with the P_0, distribution is better when starred levels are excluded from the analysis. This is particularly evident in the case of next-nearest spacing distribution (Table IX).

TABLE XI. Correlations ρ^k between level spacings D_j and D_{j+k}.

k	Th^{232}	U^{238}(part)	"Theory"
1	−0.21±0.07	−0.26±0.08	−0.25±0.03
2	−0.09±0.08	0.16±0.08	−0.11±0.03
3	0.06±0.08	−0.14±0.08	−0.03±0.03
4	−0.04±0.08	0.16±0.08	0.03±0.03
5	−0.13±0.08	0.05±0.09	0.00±0.03

The moments M^1 to M^4 of the experimental distributions of nearest- and next-nearest spacings have also been obtained and are shown in the tables. These are compared with the theoretical calculations of Porter.[26] M^k is the average of $(D/\langle D\rangle)^k$ or $(D^1/\langle D\rangle)^k$ for the experimental values of D and D^1. For the extreme case of a constant level spacing one has $M^k=1$ for the nearest-neighbor distribution and $M^k=2^k$ for the next-nearest-neighbor distribution.

The values listed as "theory" for the moments are based on Porter's results for Monte Carlo calculations using 10 000 random 10×10 matrices. The experimental occurrence of a few unexpectedly large values of D or D^1, as discussed above, would tend to make the experimental moment values larger than the predicted values. We regard the agreement between the experimental results and the theoretical predictions for an orthogonal ensemble as being generally good.

10. CORRELATION COEFFICIENTS

We have determined the values of the correlation coefficients as defined in Eq. (11), between adjacent spacings D_j and D_{j+1}, between adjacent level Γ_n^0 values, and between the Γ_n^0 for a level and the average of its spacing from the two adjacent neighboring levels. In the case of U^{238} this was done using all the resonances and again omitting the starred levels (denoted "part"). The results for the energy ranges (0–1000) eV, (0–2000) eV, (0–3000) eV, and (0–3750)eV are shown in Table X.

Table XI shows the correction coefficients ρ^k for the level spacings D_j and D_{j+k} for Th^{232} and for U^{238}. The U^{238} values are obtained excluding the starred levels. The energy region (0–3) keV was used for both elements. The last column gives the results quoted by Garrison obtained from Monte Carlo calculations of 10 000 random 10×10 matrices, and 200 random 20×20

[26] C. E. Porter, Brookhaven National Laboratory, BNL Report 6763 (unpublished).

matrices. A statistical uncertainty of ± 0.03 is given for the "theoretical" values.

The results for the adjacent spacing correlation is in good agreement with the result[17,23] for random matrices. The $(\Gamma_n^0)_j - (\Gamma_n^0)_{j+1}$ correlation of the reduced width for adjacent levels is small, and probably not inconsistant with zero. A possible experimental bias exists in that a very weak level is more apt to be missed if it is adjacent to a very strong level. No theoretical predictions other than zero have been made for this quantity to our knowledge.

The correlation of $(\Gamma_n^0)_j$ with the average of the spacings for adjacent levels seems to come out positive, but not necessarily significantly different from zero. Again an experimental bias could exist in that an isolated weak resonance is easier to observe than one close to a strong level. A positive correlation coefficient for $(\Gamma_n^0)_j$ and D_j suggests that these quantities vary in the same direction from level to level to reduce the fluctuations in the ratios $(\Gamma_n^0/D)_j$. Such an effect, to the best of our knowledge, is not expected theoretically.

11. CONCLUSION

The improved resolution of our present neutron velocity spectrometer has enabled us to determine the energies and resonance parameters of a significantly larger number of resonance levels in Th^{232} and U^{238} than has been known previously. More precise values for the s-wave strength functions, and mean level spacings have been obtained for these nuclei, which can be compared with the predictions of the theoretical models.

The statistical properties of the level spacing distribution and the correlation between spacings have been compared with the predictions of the theoretical model of real symmetric Hamiltonian matrices having randomly distributed matrix elements. The agreement of the data with the theoretical model is found to be good. The single-channel Porter-Thomas distribution for the neutron reduced widths has been tested more stringently and is found to be in good agreement with the experimental results. Further detailed tests of the theory require an order of magnitude improvement in the amount and quality of the data.

ACKNOWLEDGMENTS

The authors take great pleasure in acknowledging the invaluable cooperation of Arthur Blake, the general foreman of operations for the velocity selector and his assistants, S. Marshall, J. Spiteri, and D. Ryan. The final analysis of the data could not have been done without the skilled help of Bum-Nai Ham and Young-Hee Ham at programming and operating the digital computers. Discussions with Dr. C. E. Porter, Dr. E. Melkonian, and Dr. P. B. Kahn contributed materially to our understanding of the problems. Finally we wish to express our gratitude to the operating staff of the Nevis Synchrocyclotron, whose enthusiastic cooperation made possible the complicated operation of the neutron velocity spectrometer.

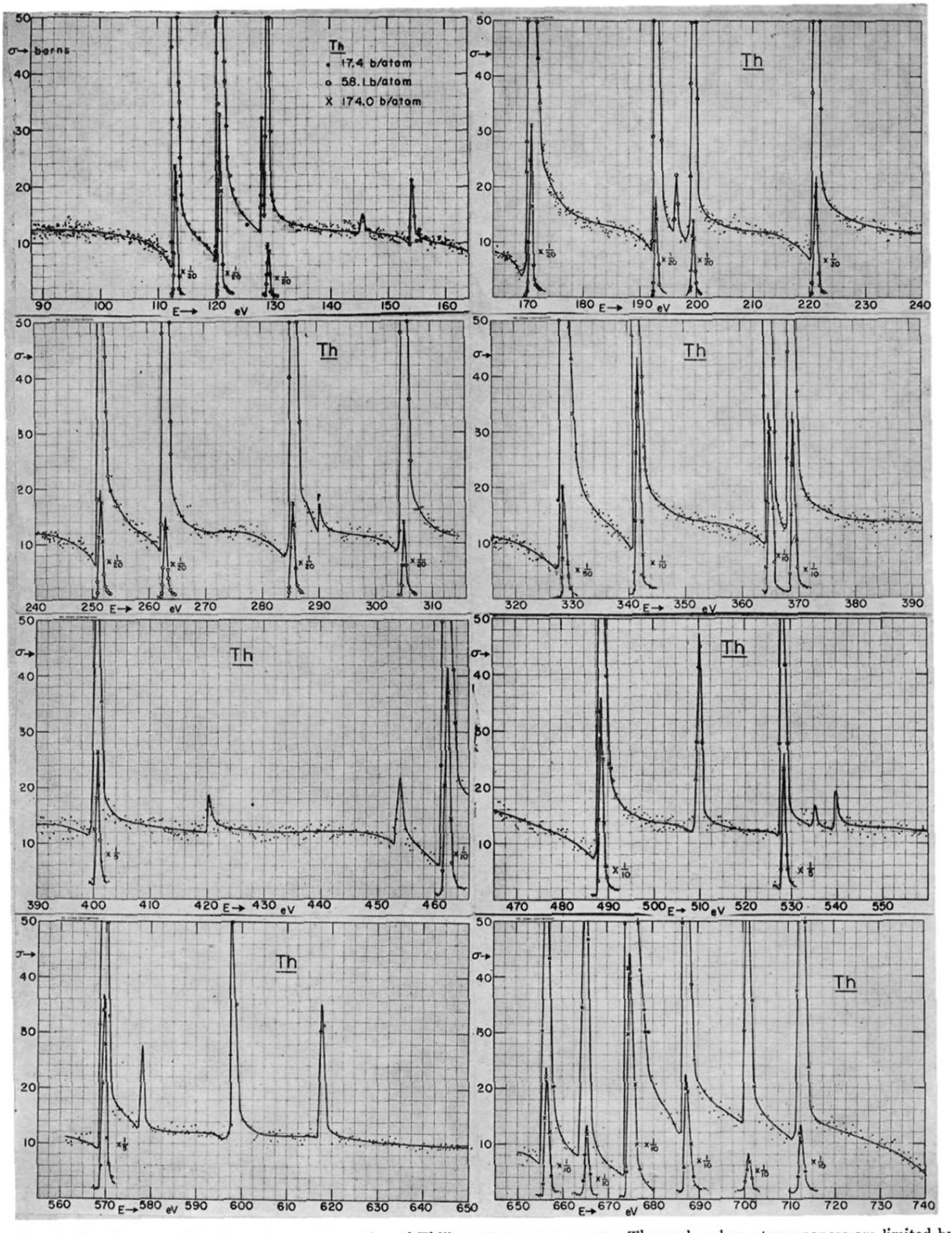

FIG. 1. The "measured" total neutron cross section of Th^{232} versus neutron energy. The peak values at resonances are limited by Doppler level broadening, experimental energy resolution, and the size of the $1/n$ value for our thinnest sample. Areas under these curves for the resonances may be quite different from the area under a true σ versus E plot.

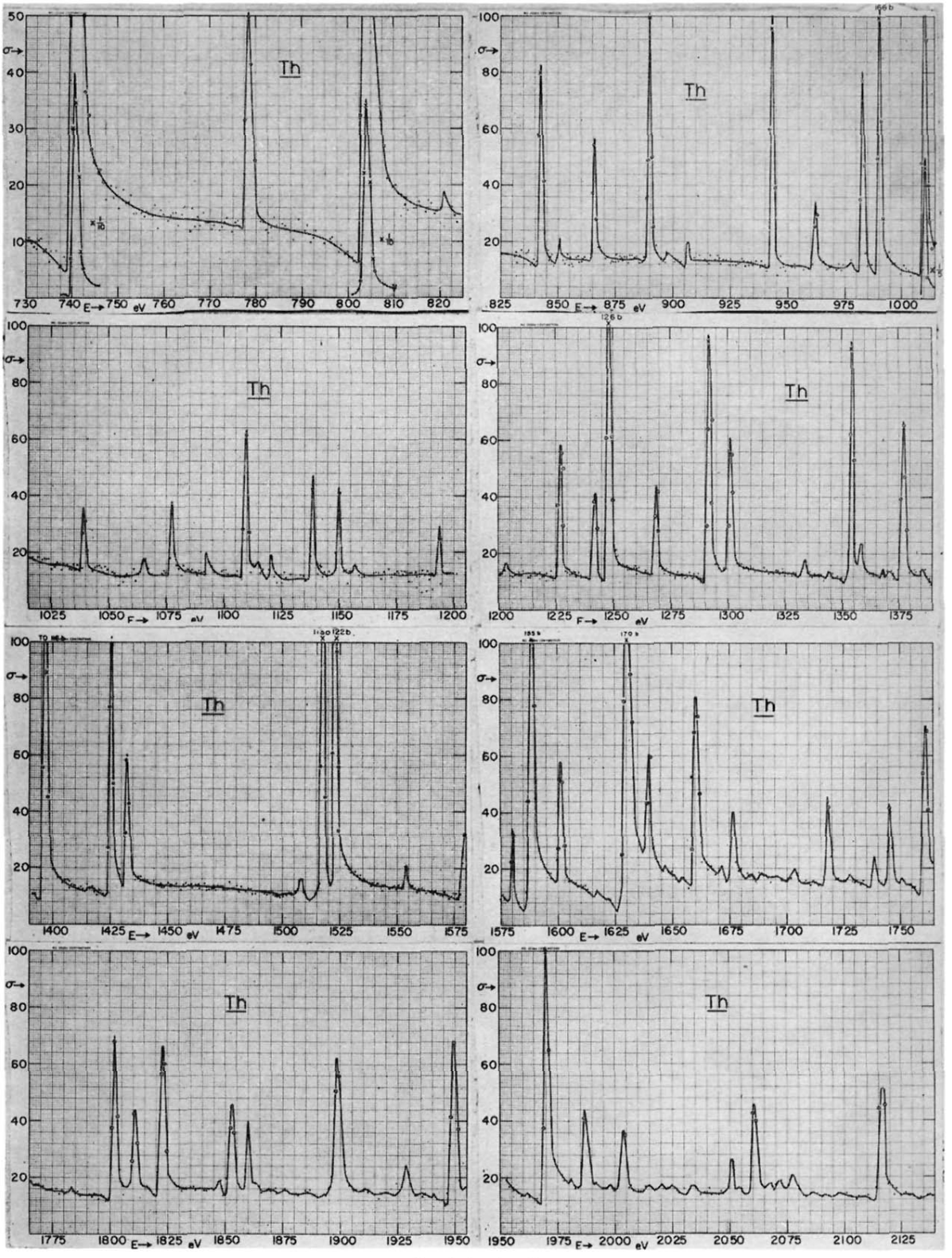

FIG. 1 (*continued*)

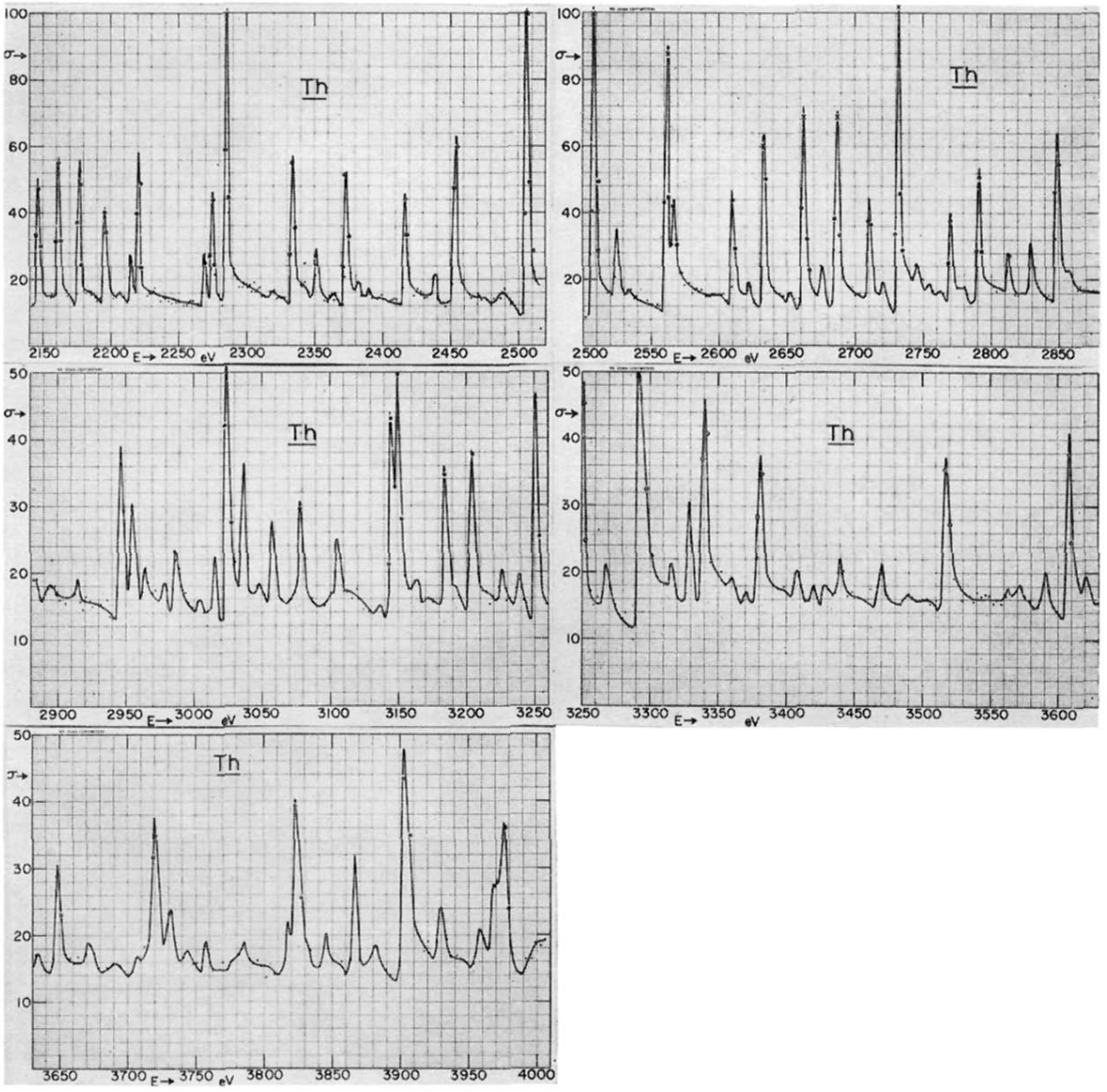

FIG. 1 (*continued*)

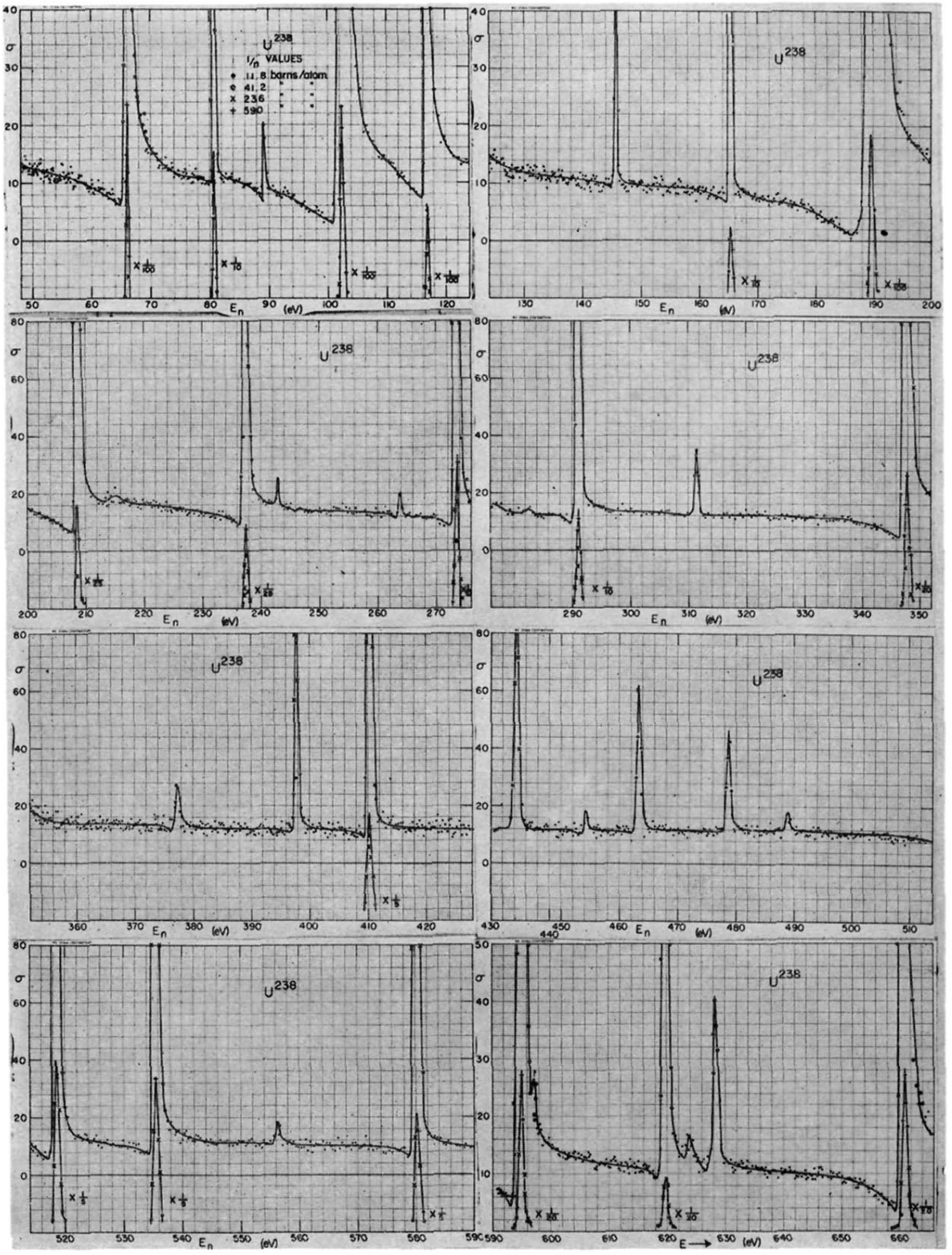

FIG. 2. The "measured" total cross section of U^{238} versus neutron energy.

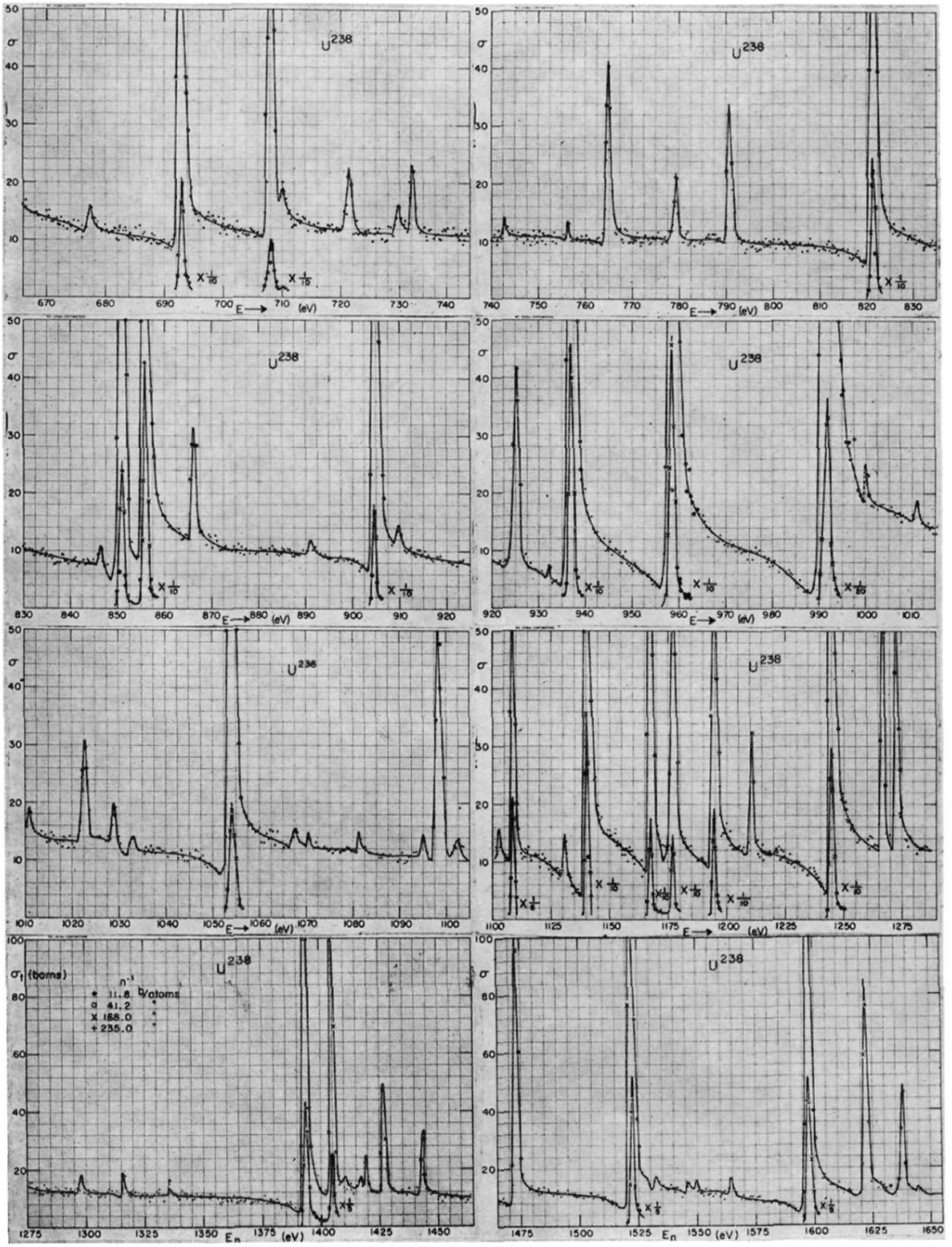

FIG. 2 (*continued*)

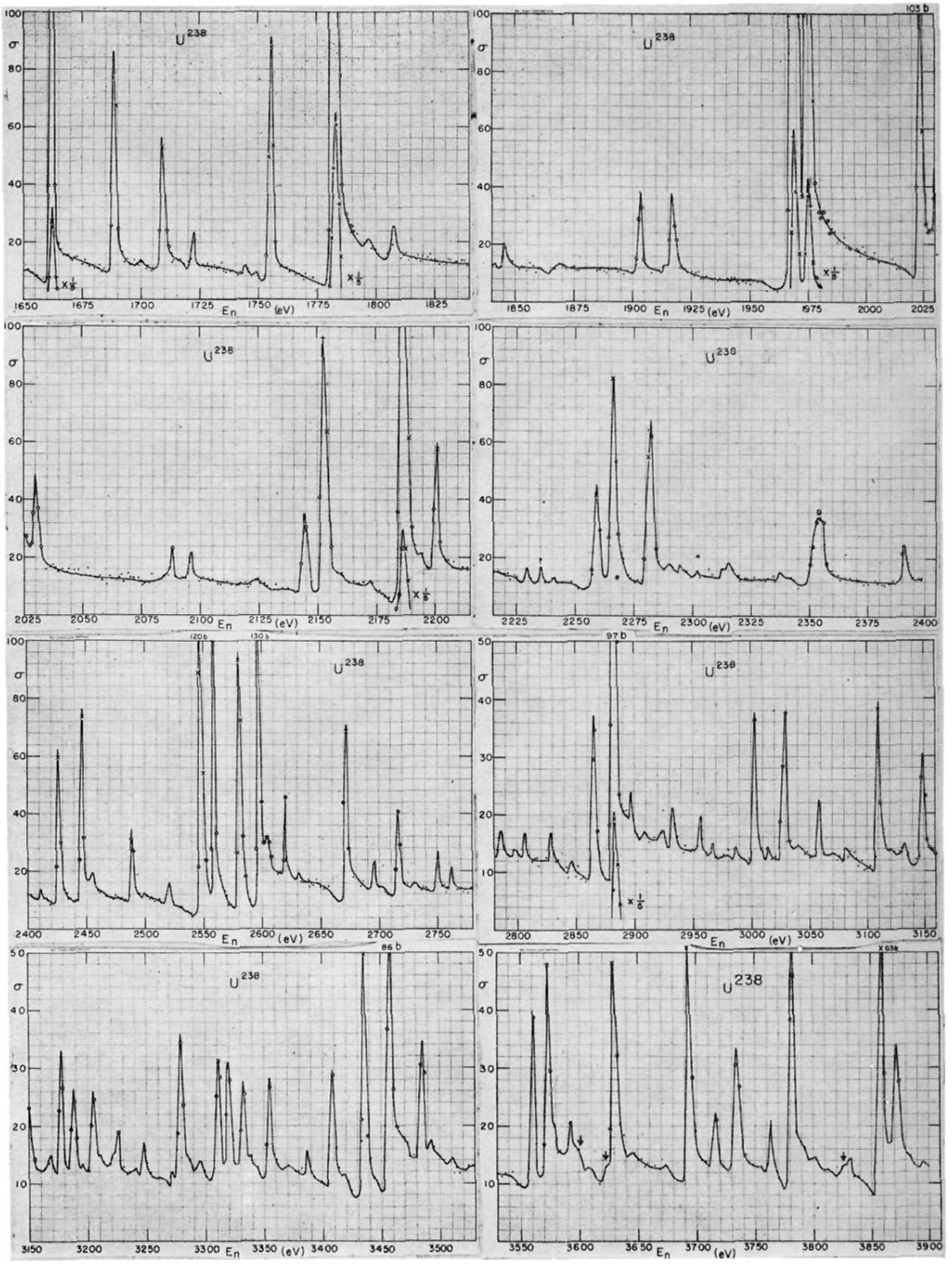

FIG. 2 (*continued*)